

## 24. X-RAY MINERALOGY STUDIES – LEG 8

H. E. Cook and I. Zemmels, University of California, Riverside, California

### INTRODUCTION

The semi-quantitative determination of mineral composition has been performed according to the methods described in the DSDP reports of Legs 1 and 2 and in Appendix III of Volume IV.

The iron oxide mineral goethite was positively identified for the first time in Deep Sea Drilling Project cores. It occurs at Sites 74 and 75 mainly in the iron- and manganese-rich sediments directly above basaltic basement. No factors were available to calculate the goethite content in the sediment; its occurrence is only qualitatively noted in the text and in the mineral concentration tables at the end of this paper.

In general, sediments from the Pacific Ocean contain large quantities of volcanic glass, biogenous opaline silica and iron-manganese colloids. These materials, which are X-ray amorphous, tend to dilute and to mask the crystalline minerals. The per cent *amorphous scattering* is a measure of the amount of amorphous material in the sample (Rex *et al.*, 1971). In samples which have a high amorphous scattering value, the number of minerals reported is apt to be small because weakly diffracting minerals and minerals in low concentrations cannot be detected. Furthermore, the precision of the semi-quantitative determination of those minerals which are detected is lower because of the reduced intensity of diffraction.

Barite was found with unprecedented frequency in sediments from Sites 69 through 74. The possibility of contamination from barite in drilling mud has been suggested, but it does not appear to be likely in this case. Drilling mud was used in coring Holes 68A and 75A, but no samples were submitted for X-ray analysis. In the case of Hole 70A, mud was used only to fill the hole for electric logging after sampling. There remains the possibility, however, that sediments recovered from holes drilled subsequently to the use of drilling mud have become contaminated by residual drilling mud left on the walls of the drill pipe. Conceivably, the core barrel could pick up residual drilling mud during its travel down the drill string. The data do not seem to indicate that contamination by this means has occurred. First, we find no relation between the amount of barite and the porosity of the sediment, the degree of induration of the sediment, the degree of disturbance of the core, nor with the position of a sample within the core barrel. Samples from the interior parts

of firm chalks as well as unconsolidated oozes contain barite. Second, a general increase in barite content with depth is observed; this is contrary to what might be expected if the drill string were being "cleaned" of drilling mud from previous holes by the travel of the core barrel. Third, if drilling mud were contaminating the sediments, a correlation should exist between barite and montmorillonite occurrence, since both of these minerals are used in the mud; however, no correlation was found.

Carbonate-free samples which were known to contain barite as the only crystalline phase were examined microscopically. In many cases, no barite crystals could be seen, thus implying that the barite crystals are typically smaller than about two microns. Occasionally a few crystals about 20 microns were seen. By contrast, the barite which is used in drilling mud on the *Glomar Challenger* has a narrow size range between 10 and 40 microns.

Attempts to beneficiate the barite in natural samples by heavy liquid separation failed to yield any barite. This suggests that the barite in the samples is highly complexed with the less dense sedimentary materials and is floated off. Artificial mixtures of barite and sediment, however, did yield barite. The complexed, fine-grained nature of the barite in the samples combined with the small likelihood of contamination in the drilling process favor the explanation that the barite is of a natural origin.

In the tables of results of X-ray diffraction analysis (Tables 1 to 8) dashes (—) are used to indicate that a mineral was not detected. The dashes replace the designation 00.0 per cent which was used in all previous X-ray mineralogy reports.

No semi-quantitative determinations of the mineral concentrations were made for the silt fractions ( $2-20\mu$ ). Instead, selected minerals which commonly have an authigenic origin were sought, and are reported in Tables 1 to 8 on a ranked scale. The minerals sought were: barite, phillipsite, clinoptilolite, erionite, dolomite, siderite, rhodochrosite, goethite, hematite, magnetite, cristobalite, pyrite and apatite. The minerals were ranked according to whether they constitute the major crystalline phase present (M), whether they are present (P), or whether they are present in trace (barely detectable) amounts (T).

The X-ray mineralogy results are discussed in the framework of the lithostratigraphic units developed for the equatorial Pacific by Tracey *et al.* (this volume). Site 68 lies outside the area where these units were defined.

## RESULTS

### Site 68

Only the uppermost 15 meters of sediment was cored at this site. This sediment is a uniform dusky brown zeolitic clay of Middle Eocene age. Phillipsite and clinoptilolite make up more than half of the crystalline minerals identified (Figure 1). Kaolinite is the quantitatively important clay mineral in the bulk sample, but mica and montmorillonite are dominant in the clay fraction (Figure 2).

Chert was recovered at 9 meters and 15 meters below the sea floor, but no samples were submitted for X-ray analysis.

### Site 69

At this site the Clipperton Oceanic Formation is Miocene in age and is divided into an upper radiolarian ooze and a lower cyclic unit consisting of interbedded radiolarian ooze and radiolarian-calcareous nannofossil ooze. The high percentage of amorphous scattering in this formation (Figures 3 and 4; Table 2) is largely due to opal. In both units quartz, K-feldspar, plagioclase, kaolinite occur in similar proportions in the bulk fraction. Mica is the quantitatively important clay mineral. The occurrence of barite is virtually restricted to the silt-size fraction.

The Marquesas Oceanic Formation is composed mainly of calcareous nannofossil ooze and contains only small amounts of radiolarian ooze. Its age is Oligocene and Miocene at this site. The bulk mineralogy of this formation is characterized by a high calcite content and a very low content of clay and felsic minerals (Figures 3 and 5). This contrasts sharply with the overlying, highly opaline Clipperton Oceanic Formation. Barite is common, and increases with depth in the less than 2-micron fraction (Figure 6). Montmorillonite is the dominant clay mineral throughout this formation (Figure 6). Quartz and kaolinite are ubiquitous.

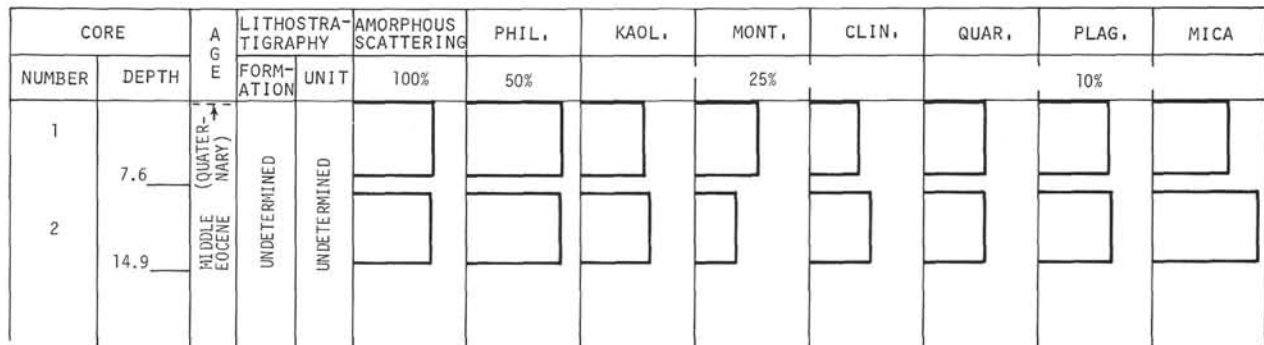


Figure 1. Site 68. Bulk.

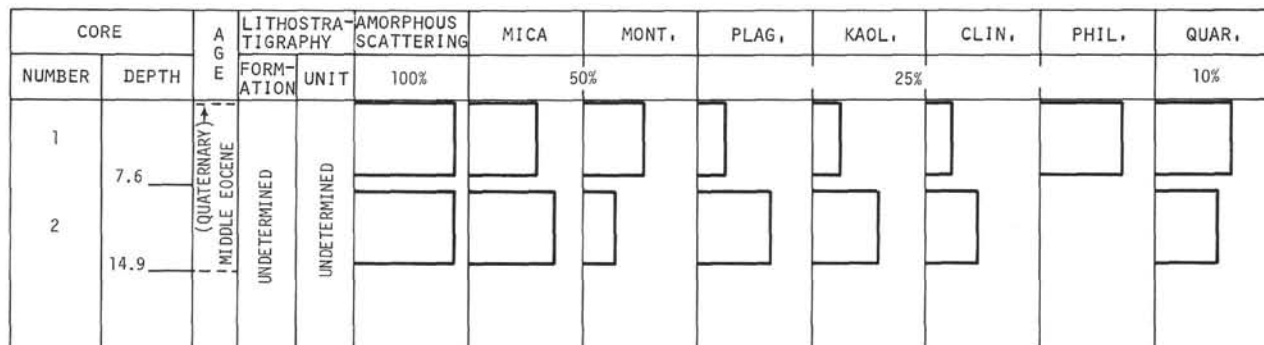


Figure 2. Site 68. Less than 2 $\mu$ .

The Line Islands Oceanic Formation is Middle and Late Eocene in age and consists of a brown radiolarian ooze. Drilling was terminated at 231 meters in Middle Eocene sediments containing chert. This chert was not submitted for X-ray analysis. The mineral content is highly variable in the Line Islands Formation with montmorillonite the dominant clay mineral (Figures 3 to 6). Barite is very abundant, even forming the major crystalline component in some bulk samples (Figure 5 and Table 2).

#### Site 70

The Clipperton Oceanic Formation is Middle Miocene to Quaternary age at this site and consists of a radiolarian ooze unit and a cyclic unit, as at Site 69. The cyclic unit is highly calcareous (Figure 7). The only major occurrence of chlorite on Leg 8 is found at this site (Figure 8) and is restricted to the radiolarian ooze unit (Late Miocene to Quaternary). The kaolinite content is larger in the cyclic unit (Middle Miocene) than in the radiolarian ooze unit. Barite appears to be largely restricted to the coarser sizes in both units (Table 3). The only occurrence of phillipsite at this site was found in the bulk fraction of the radiolarian ooze unit.

The highly calcareous Marquesas Oceanic Formation ranges in age from Early Oligocene through Early Miocene. Montmorillonite is the dominant clay mineral and mica, quartz, kaolinite and K-feldspar occur scattered throughout (Figures 9 and 10). Barite was found in virtually every silt-size and less than 2-micron sample analyzed.

The Eocene Line Islands Oceanic Formation is more siliceous than the Marquesas Formation. Drilling terminated in a cristobalite chert bed. Montmorillonite is the only clay mineral found (Figures 9 to 12).

#### Site 71

The entire section is highly calcareous; sporadic siliceous beds are found only in the cyclic unit of the Clipperton Formation and in the Line Islands Formation. Barite is present in the clay and silt fractions throughout the section and appears to increase with depth (Figure 14 and Table 4).

At this site, the Clipperton Formation consists of a Pliocene and Pleistocene cyclic unit and a Miocene varicolored unit. In general, the cyclic unit appears to be more calcareous than at Sites 69 and 70. This probably reflects a smaller radiolarian content at Site 71. Mineralogically, the less than 2-micron fractions of the two Clipperton units are very similar (although barite is probably more abundant in the lower unit). Mica and montmorillonite are the major clay minerals. Kaolinite and K-feldspar persist throughout the Clipperton Formation in minor amounts (Figure 14).

The Marquesas Formation is Early Miocene and Oligocene in age. The contact between the Clipperton and Marquesas Formations is gradational, and correspondingly no sharp breaks in the mineral assemblages were seen. In the Marquesas Formation plagioclase is fairly uniformly distributed, while mica diminishes with depth. Kaolinite and K-feldspar are found only at the top of the formation.

The Line Islands Formation was not sampled for X-ray analysis at this site; however, it contains Late Eocene limestones with chert intergrowths.

#### Site 72

The entire section is highly calcareous; siliceous sediment occurs only in the Line Islands Formation. Barite occurs throughout the section and is most abundant in the silt fraction (Table 5).

As at Site 71, the Clipperton Formation consists of a cyclic unit and a varicolored unit. Its age is Middle Miocene to Quaternary. There are no obvious mineralogical differences between the two units (Figures 15 to 18). Mica is the dominant clay mineral. Kaolinite and K-feldspar occur throughout the cyclic unit whereas the varicolored unit only contains these minerals at the top (Figures 16 and 18).

Mineralogically the Marquesas Formation, which is Oligocene and Miocene in age, does not differ greatly from the Clipperton Formation except for slightly higher contents of quartz and montmorillonite (Figure 16).

The Line Islands Formation is of Early Oligocene age at the top. It is more siliceous than the overlying formations owing to a higher content of Radiolaria. Montmorillonite is the predominant mineral in the crystalline phases. Minor amounts of barite, plagioclase, K-feldspar, kaolinite, and quartz occur. Drilling terminated in Late Eocene sediments containing black chert. The chert was not submitted for X-ray analysis.

#### Site 73

The entire section is highly calcareous. Barite is common throughout (Figures 19 and 20; Table 6).

The Clipperton Oceanic Formation consists of a cyclic unit, a varicolored unit and a radiolarian ooze unit. It ranges in age from Middle Miocene through Pleistocene. The mineralogy of the less than 2-micron fraction in the Clipperton Formation is highly variable among samples and, consequently, no unique mineral assemblages can be ascribed to any of the units. A single occurrence of phillipsite was found in the bulk fraction of the radiolarian ooze unit.

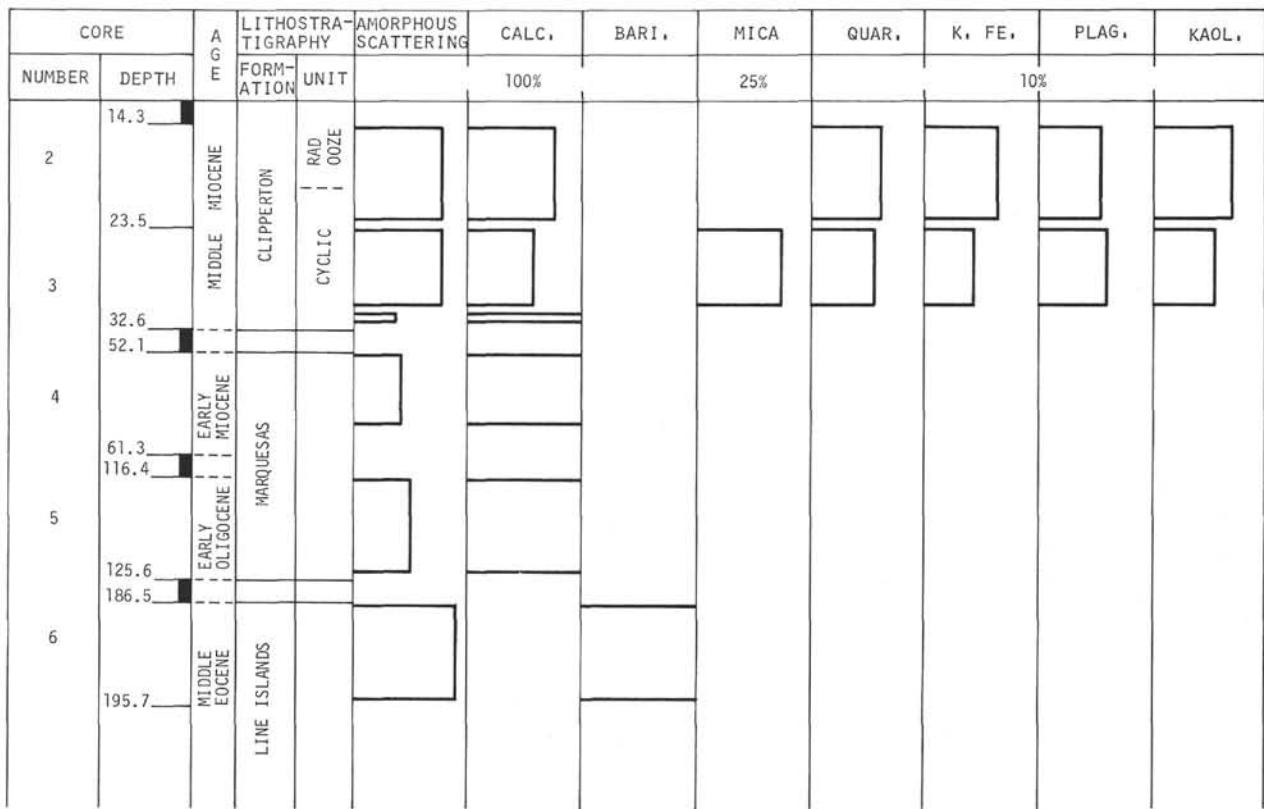


Figure 3. Site 69. Bulk.

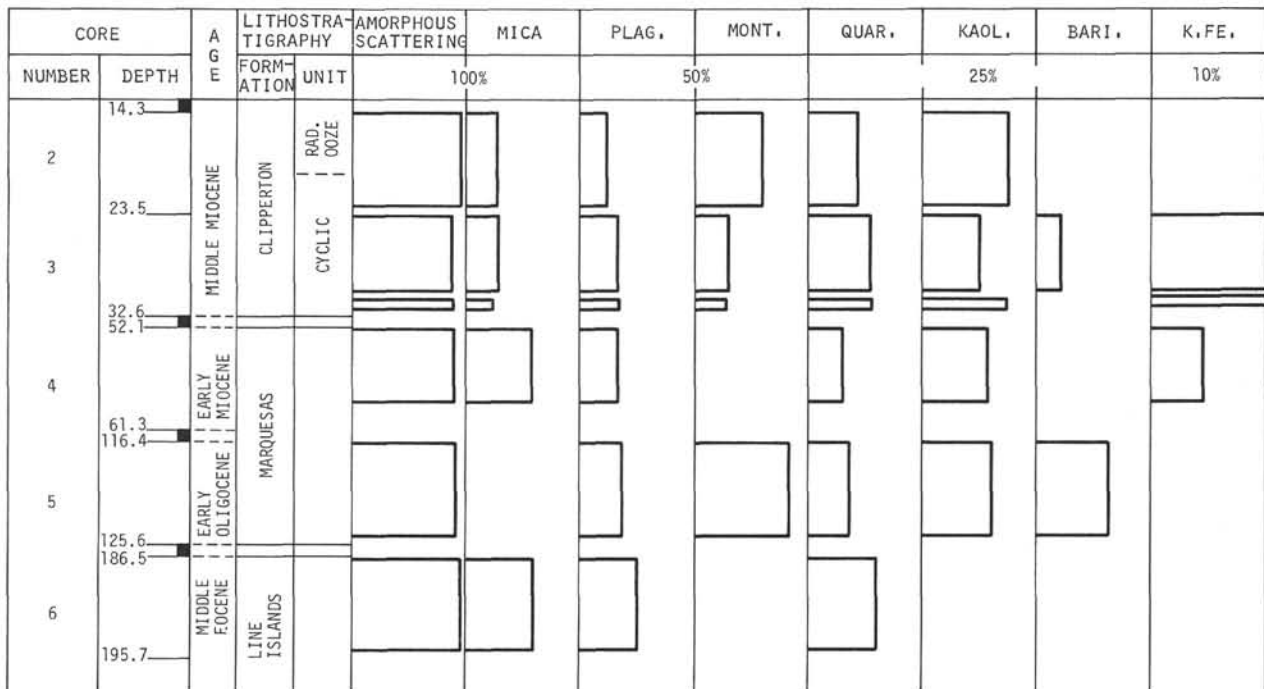


Figure 4. Site 69. Less than 2 $\mu$ .

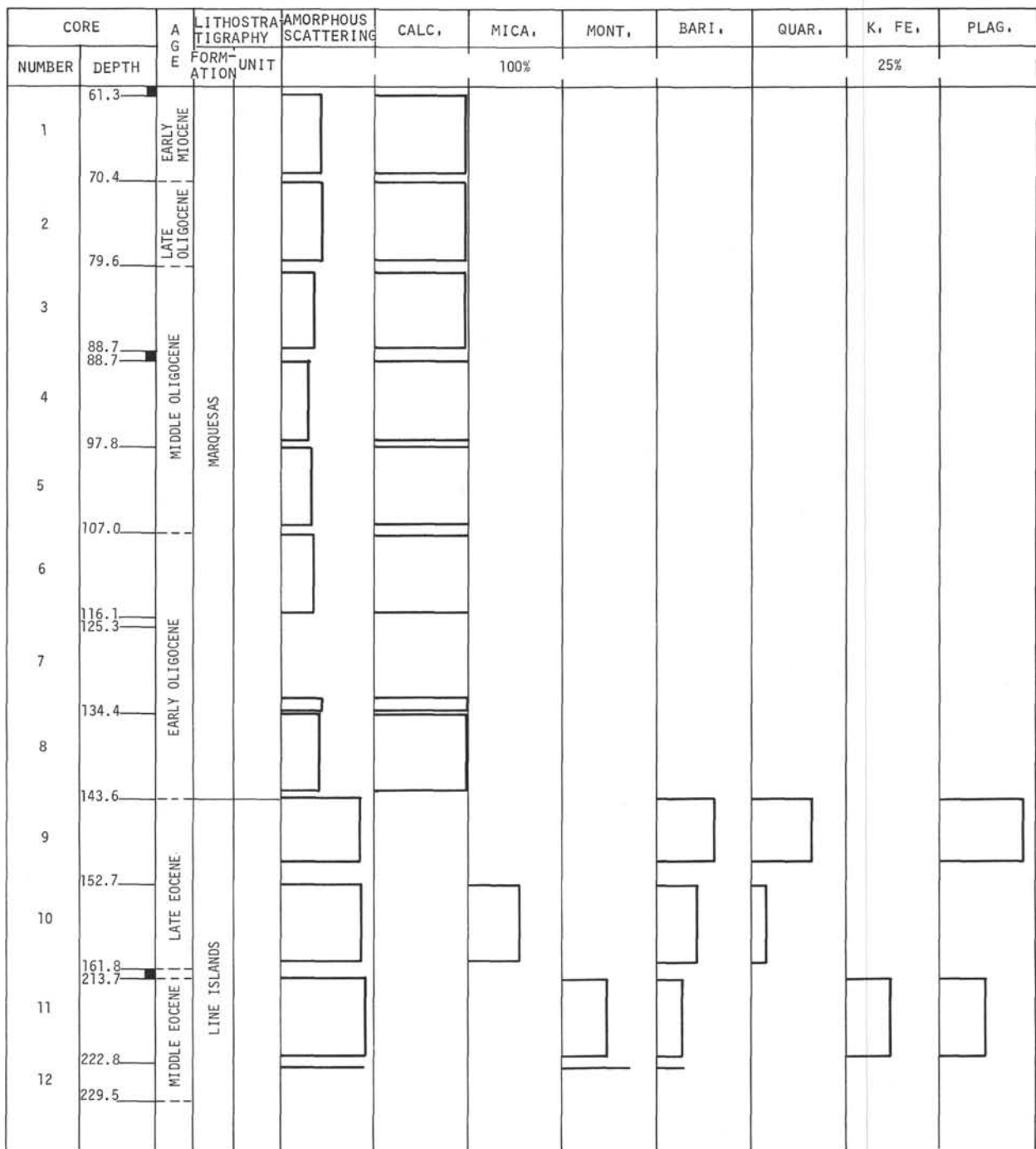


Figure 5. Site 69A. Bulk.

The Marquesas Oceanic Formation, which is Oligocene and Miocene in age, has a highly uniform mineral content with a tendency for montmorillonite and mica to vary inversely in abundance (Figure 20). Quartz, plagioclase, kaolinite and barite occur in similar concentrations throughout.

The Eocene Line Islands Oceanic Formation is somewhat more siliceous than the overlying formations. Mica and montmorillonite are the dominant minerals in the clay fraction. Also, subordinate amounts of quartz, plagioclase, kaolinite and barite occur.

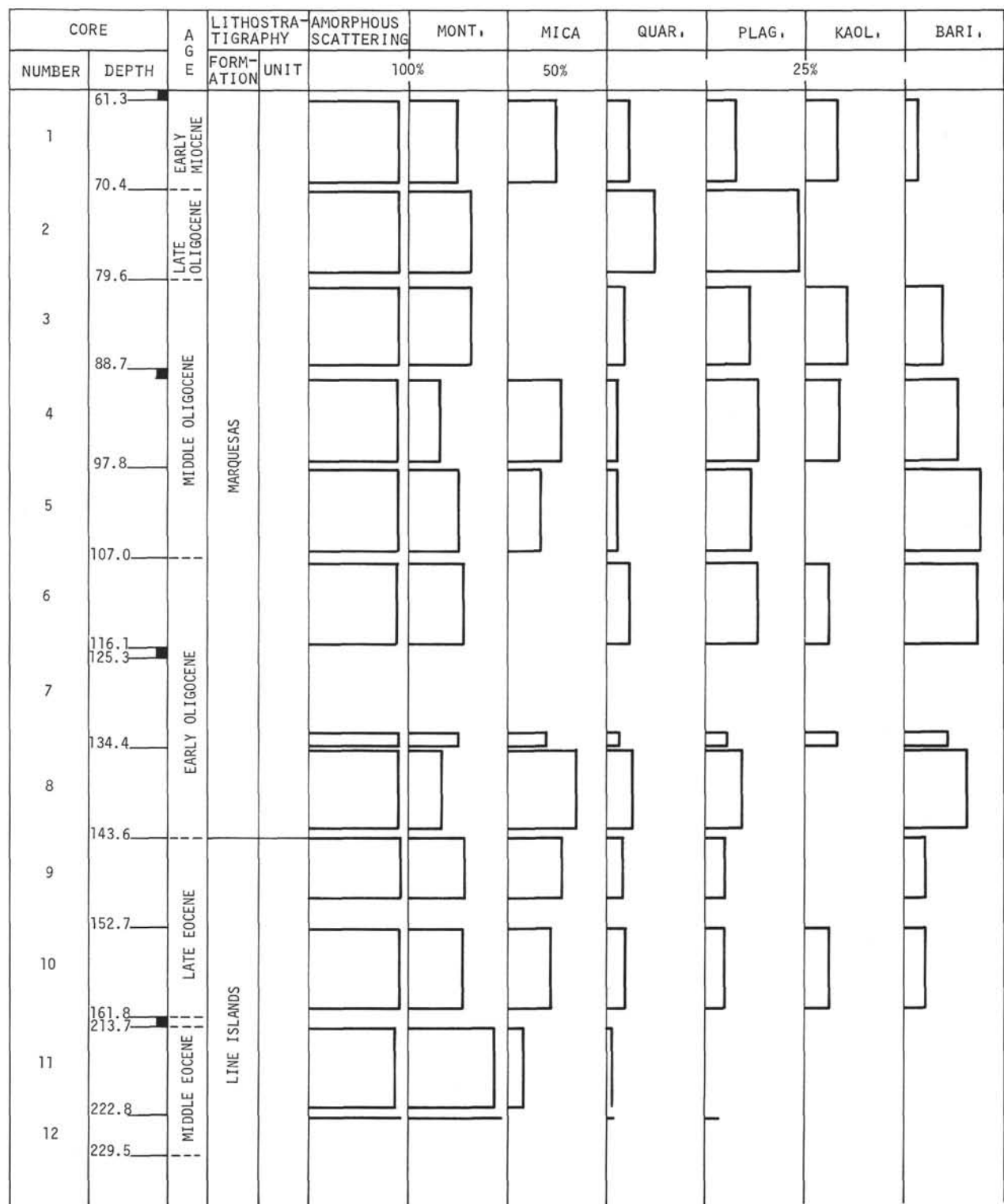


Figure 6. Site 69A. Less than  $2\mu$

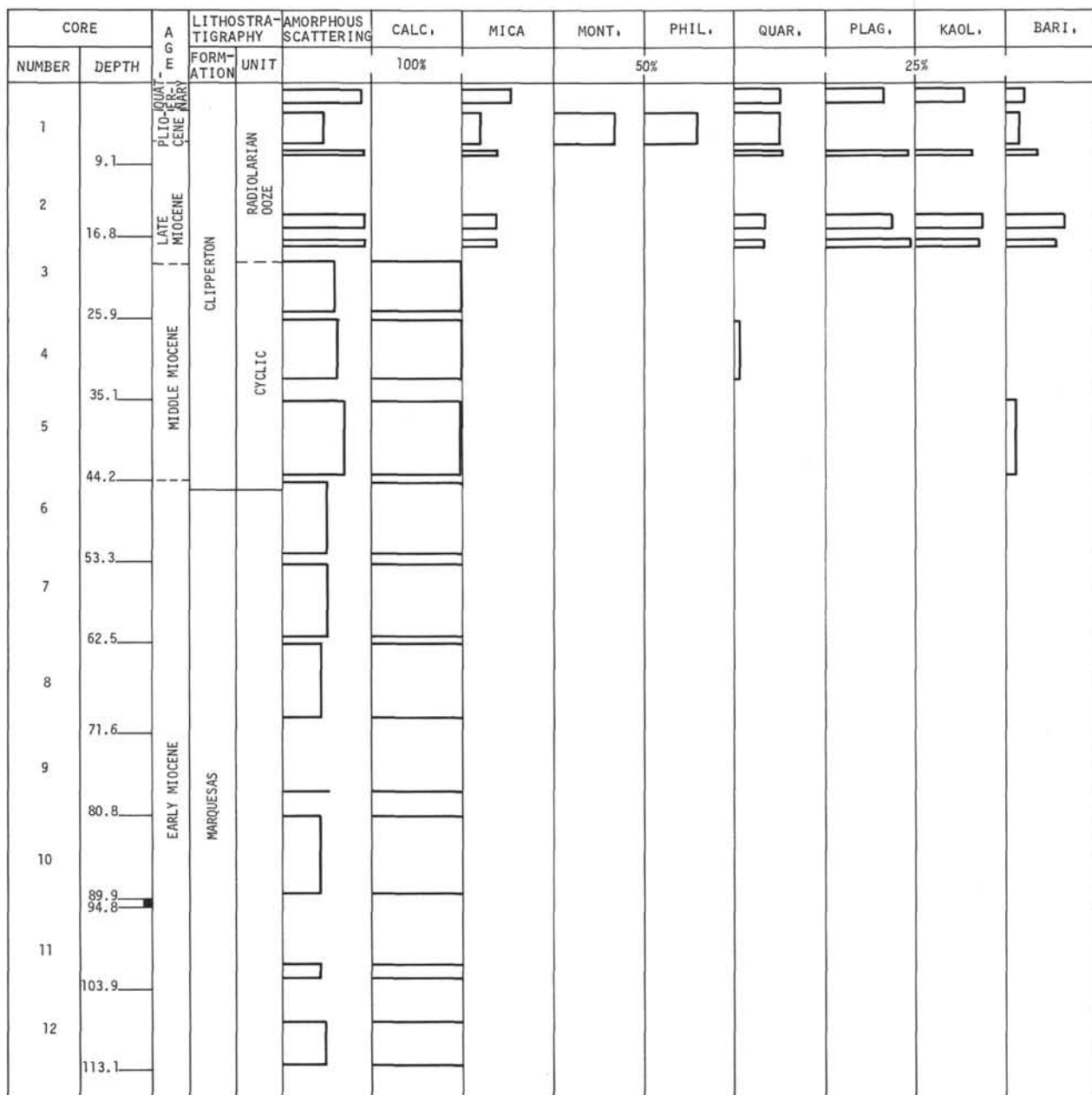


Figure 7. Site 70. Bulk.

#### Site 74

At this site the Clipperton Formation is Miocene and Pliocene in age and consists entirely of a dark brown radiolarian ooze unit. This unit is highly X-ray amorphous owing in large part to the presence of radiolarian tests and amorphous iron oxide particles. Mica and montmorillonite are the dominant clay minerals; kaolinite occurs in subordinate amounts (Figures 22 and 23). Phillipsite occurs in the Middle and Late Miocene

parts of these radiolarian oozes. Barite occurs throughout this unit in the bulk fraction but was not detected in the silt and clay fractions (Figures 21 and 22; Table 7).

The Marquesas Formation, which is Oligocene to Middle Miocene in age, is highly calcareous. Montmorillonite and mica are the dominant clay minerals; kaolinite diminishes with depth. A highly amorphous, dark brown layer, which is 1-meter thick, occurs at the

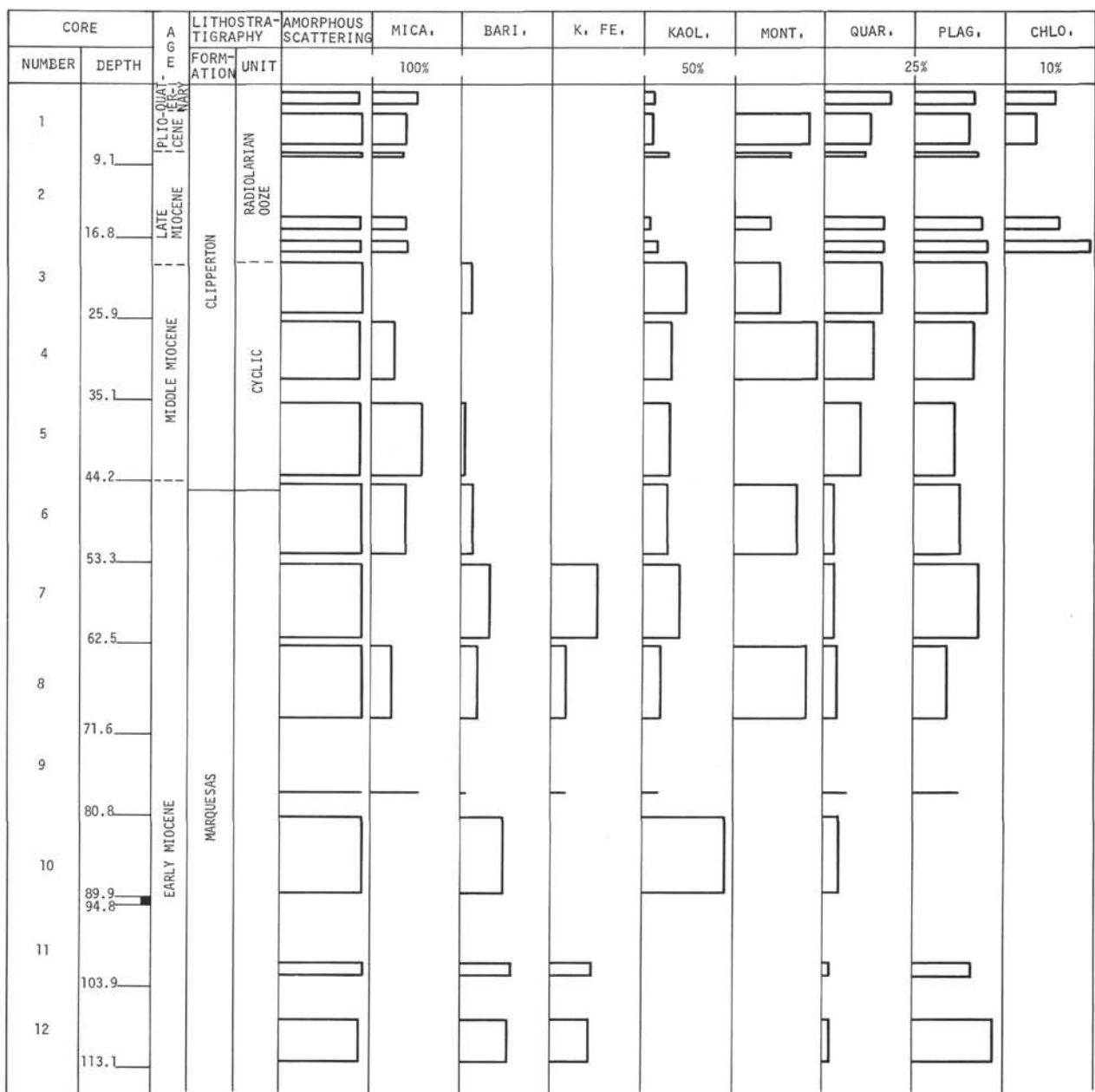


Figure 8. Site 70. Less than  $2\mu$ .

27 meter level. The layer contains amorphous iron oxides, phillipsite, and barite (Figure 21). Clinoptilolite constitutes the major crystalline phase of the silt fraction in the lower parts of the formation (Table 7).

The Line Islands Formation is a brown, calcareous, zeolitic clay which overlies glassy basaltic rock. At this site the Line Islands Formation is Eocene in age. Phillipsite and clinoptilolite occur in the silt and in the less than 2-micron fractions. Poorly crystalline goethite is present in detectable amounts in the silt and in the less than 2-micron fractions (Table 7).

#### Site 75

A thin (1.3 meter), brown, phillipsite-rich clay of Quaternary age overlies the Marquesas Formation.

The Marquesas Formation, which is Early Oligocene through the Early Miocene in age, rests directly on basaltic basement at this site. The formation consists of a brown calcareous ooze which becomes darker brown with depth. This brown color is due to the presence of amorphous iron-manganese material and goethite. Goethite is the dominant mineral in some of the deepest

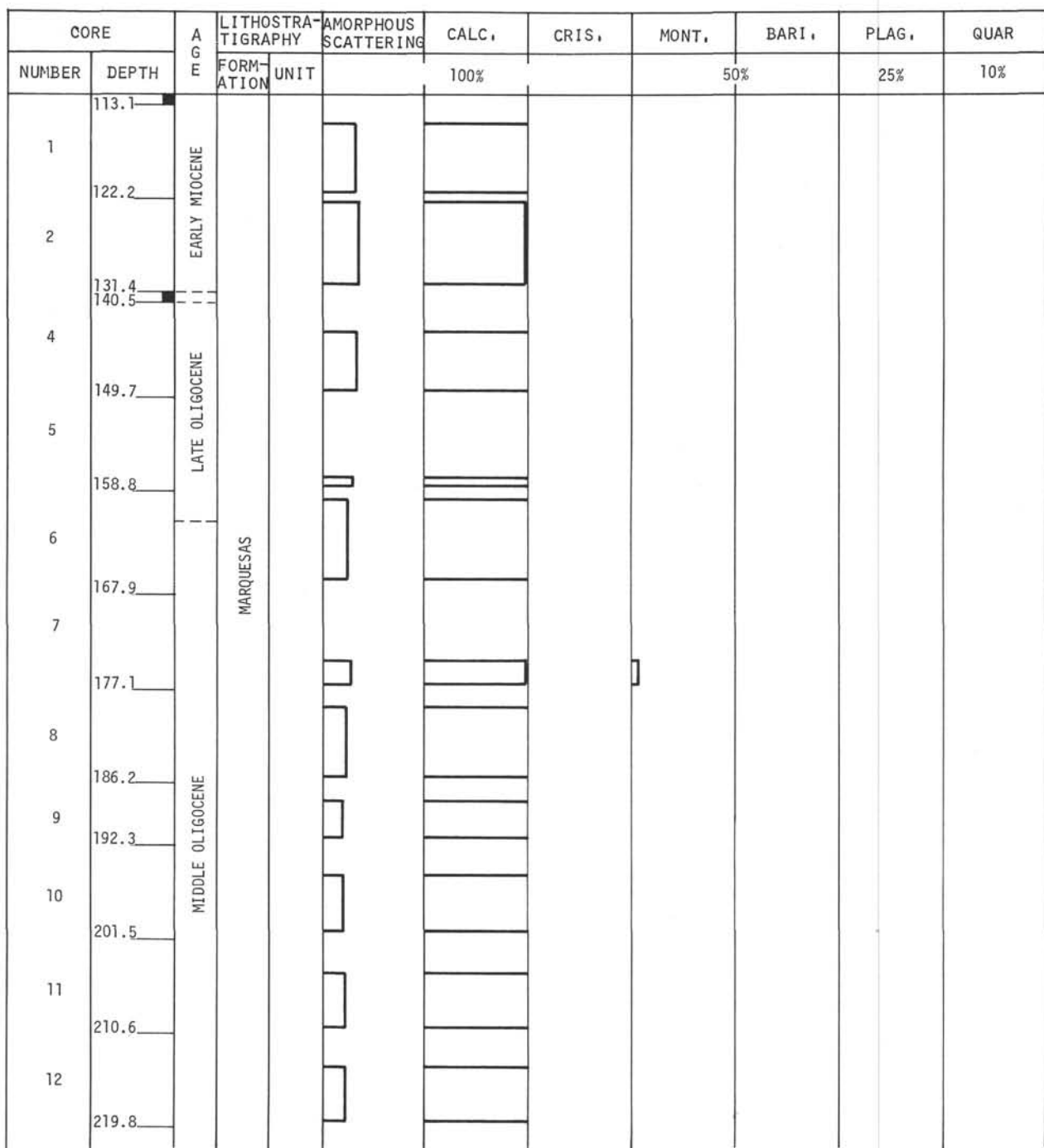


Figure 9. Site 70A. Bulk.

decalcified samples (Table 8). Phillipsite is scattered throughout the hole. Clinoptilolite occurs in the lower parts of the formation (Table 8; Figures 23 and 24). Mica is a dominant clay mineral (Figure 24) and kaolinite is always present. Montmorillonite appears to be absent at this site, but this may be due to the masking and diluting effect of the amorphous iron-manganese materials.

#### DISCUSSION AND CONCLUSIONS

The radiolarian ooze and cyclic units of the Clipperton Oceanic Formation are readily distinguished from the other stratigraphic units in bulk samples by their high amorphous scattering percentages. They generally consist of dusky brown sediments. The amorphous material consists dominantly of radiolarian tests and lesser

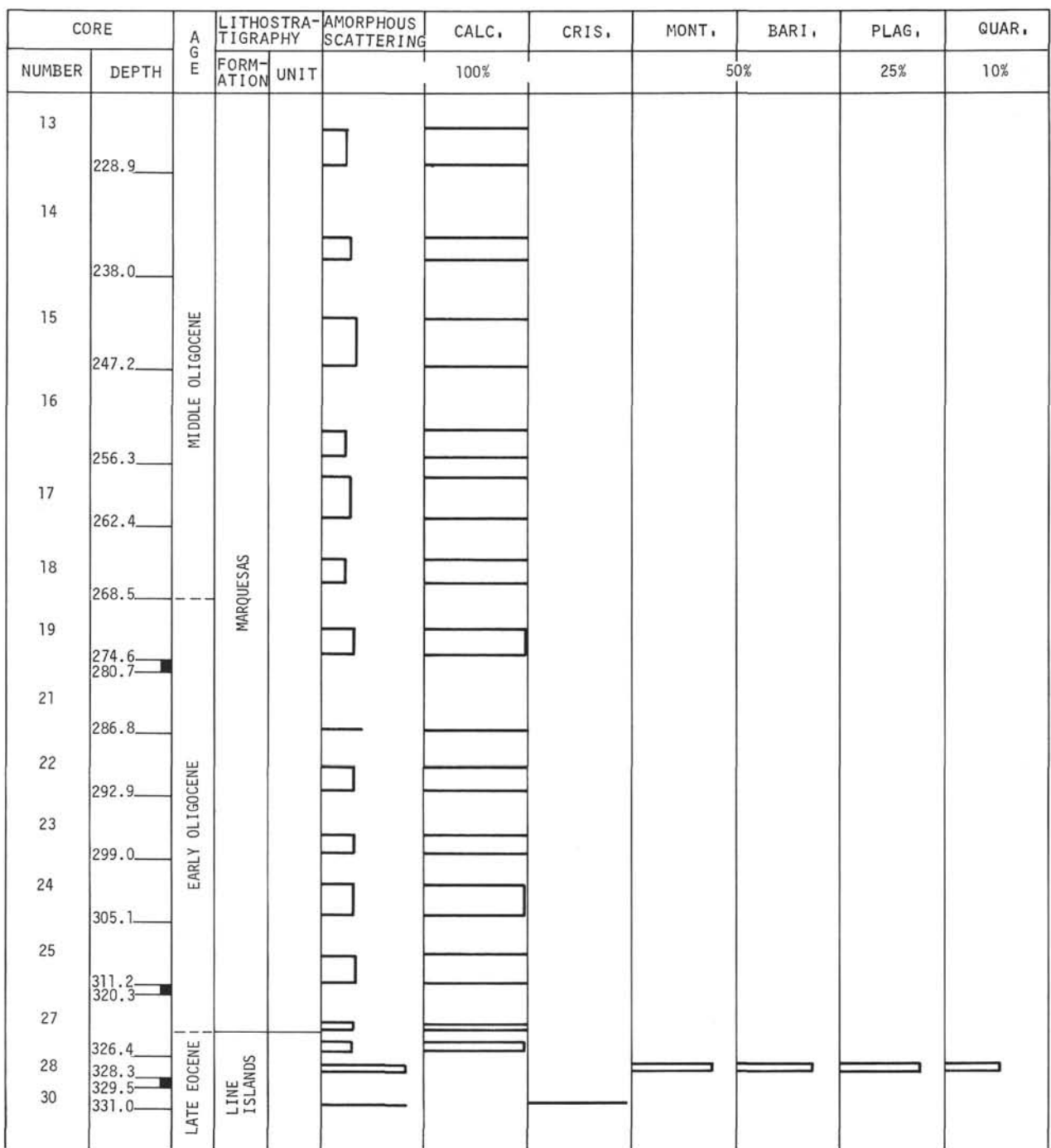


Figure 9. *Continued.*

amounts of amorphous iron oxide the latter of which gives the units their brown color. A correlation exists between the amorphous scattering percentage of these units and latitude. The three sites closest to the equator (Sites 71, 72 and 73) have lower amorphous scattering values in the radiolarian ooze and cyclic units than the three sites further north or south of the

equator (Sites 69, 70 and 74) (Figures 3, 7, 13, 15, 19 and 21). This is possibly due, at least in part, to a higher content of amorphous iron oxides at Sites 69, 70 and 74, as suggested by the reported darker brown colors at these sites. Whether or not there is also an increase of opaline silica at these sites is not known. One explanation for a latitudinal control is that the

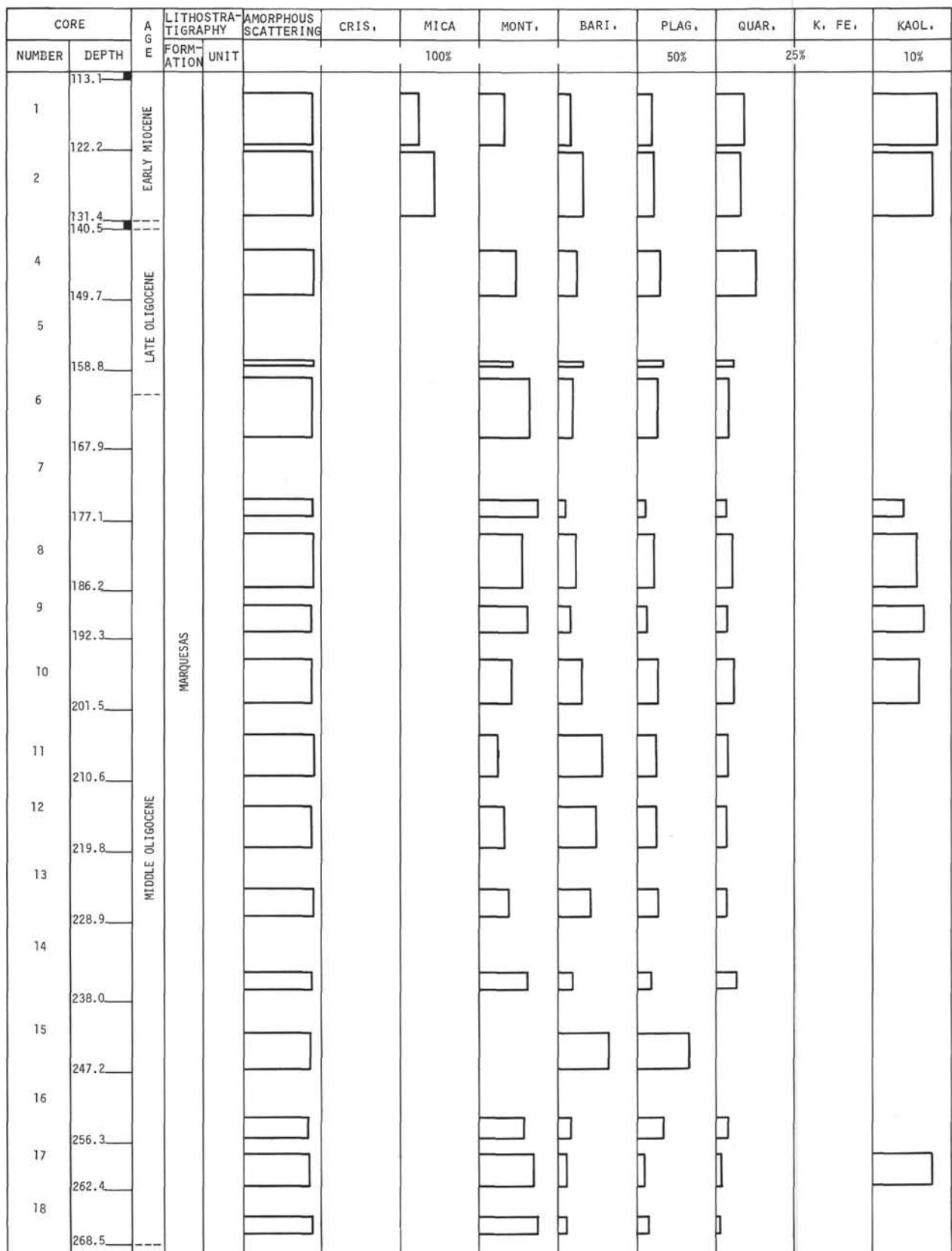


Figure 10. Site 70A. Less than 2 $\mu$ .

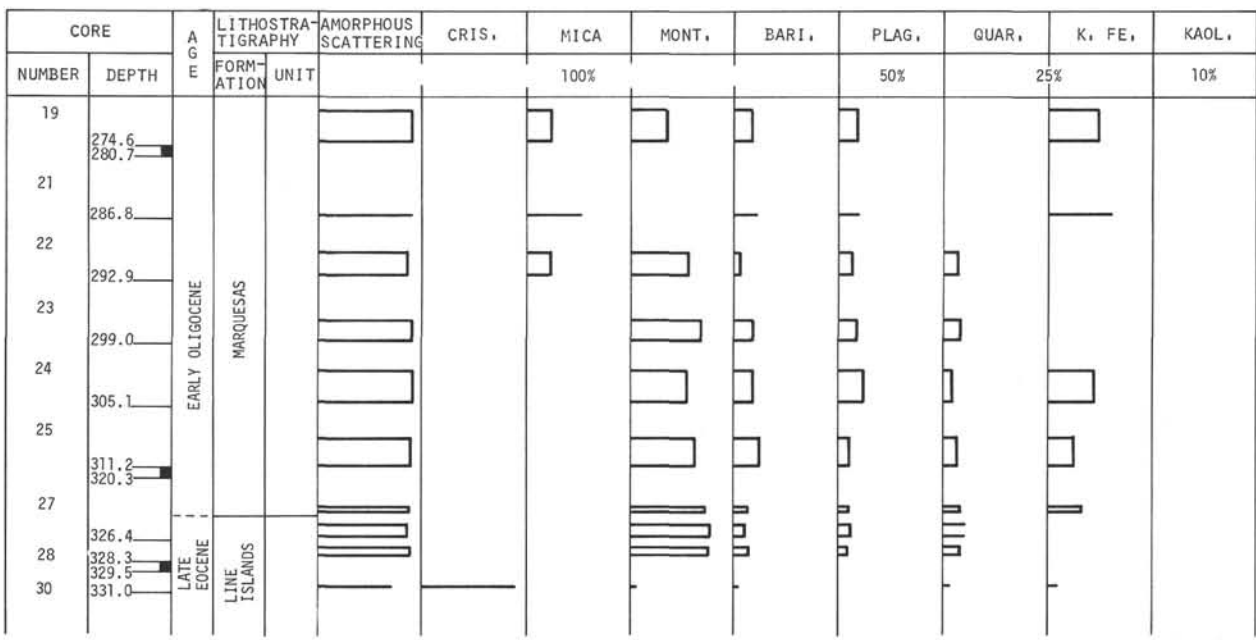


Figure 10. *Continued.*

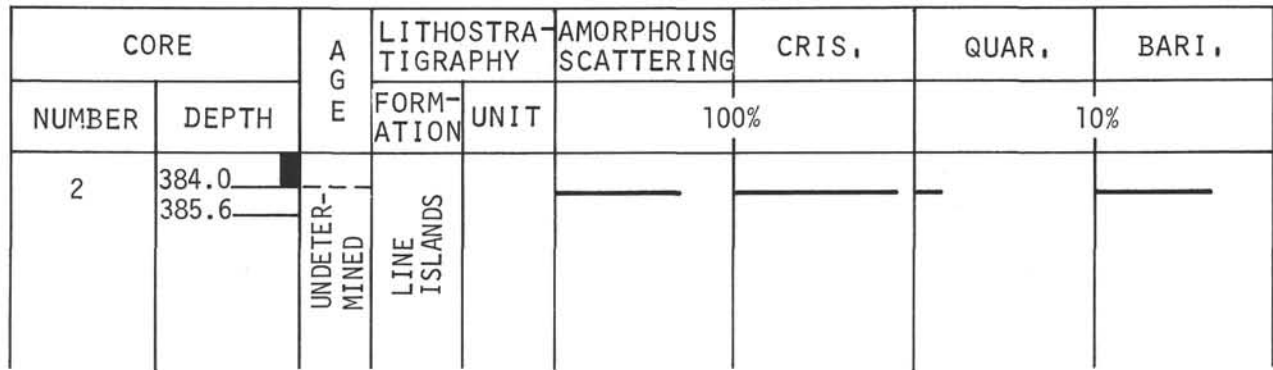


Figure 11. Site 70B. Bulk.

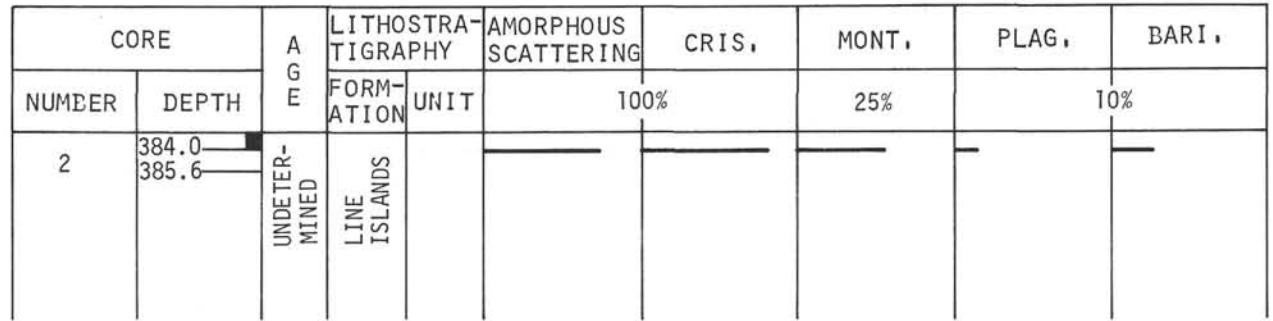


Figure 12. Site 70B. Less than 2 $\mu$ .

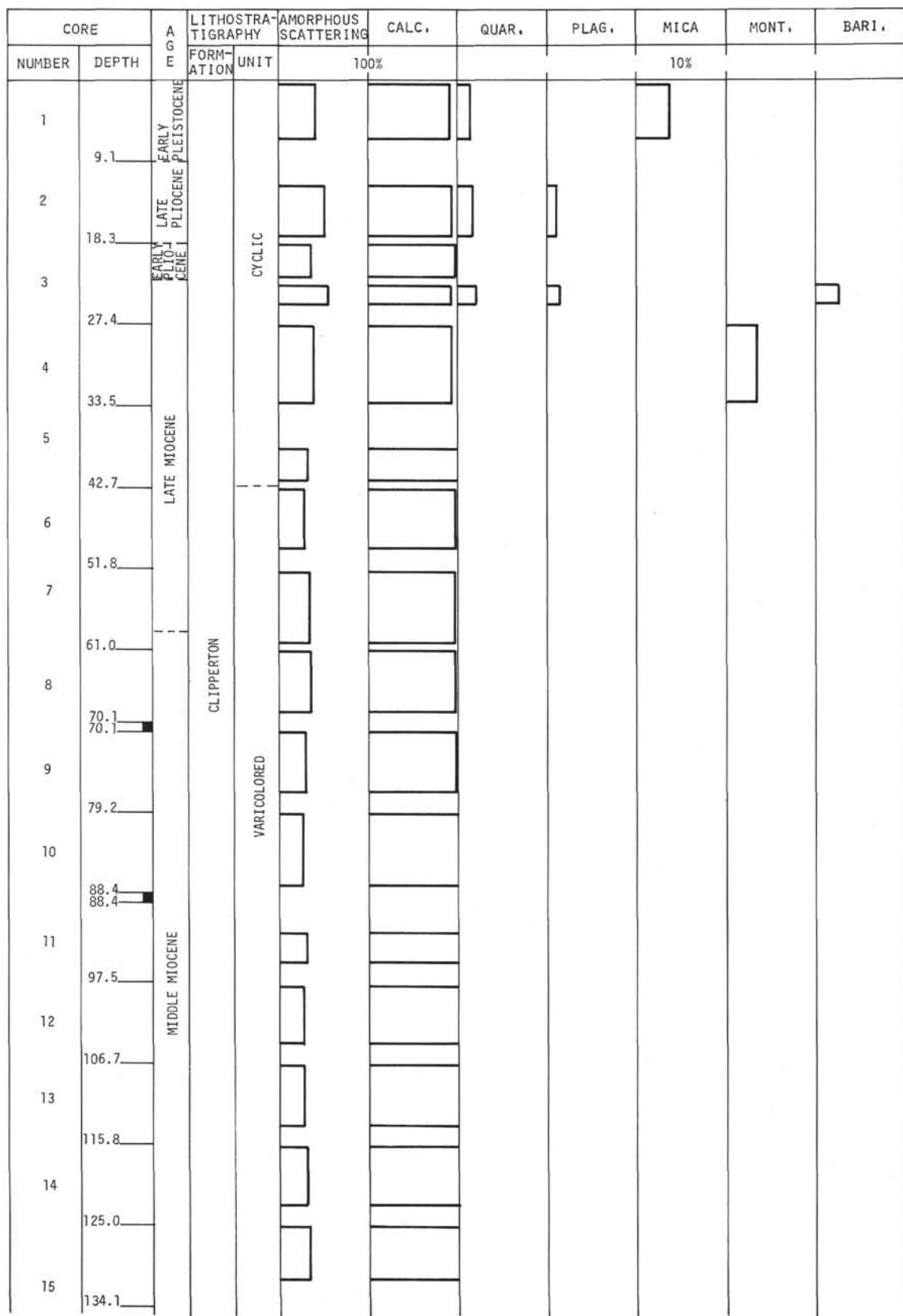


Figure 13. Site 71. Bulk.

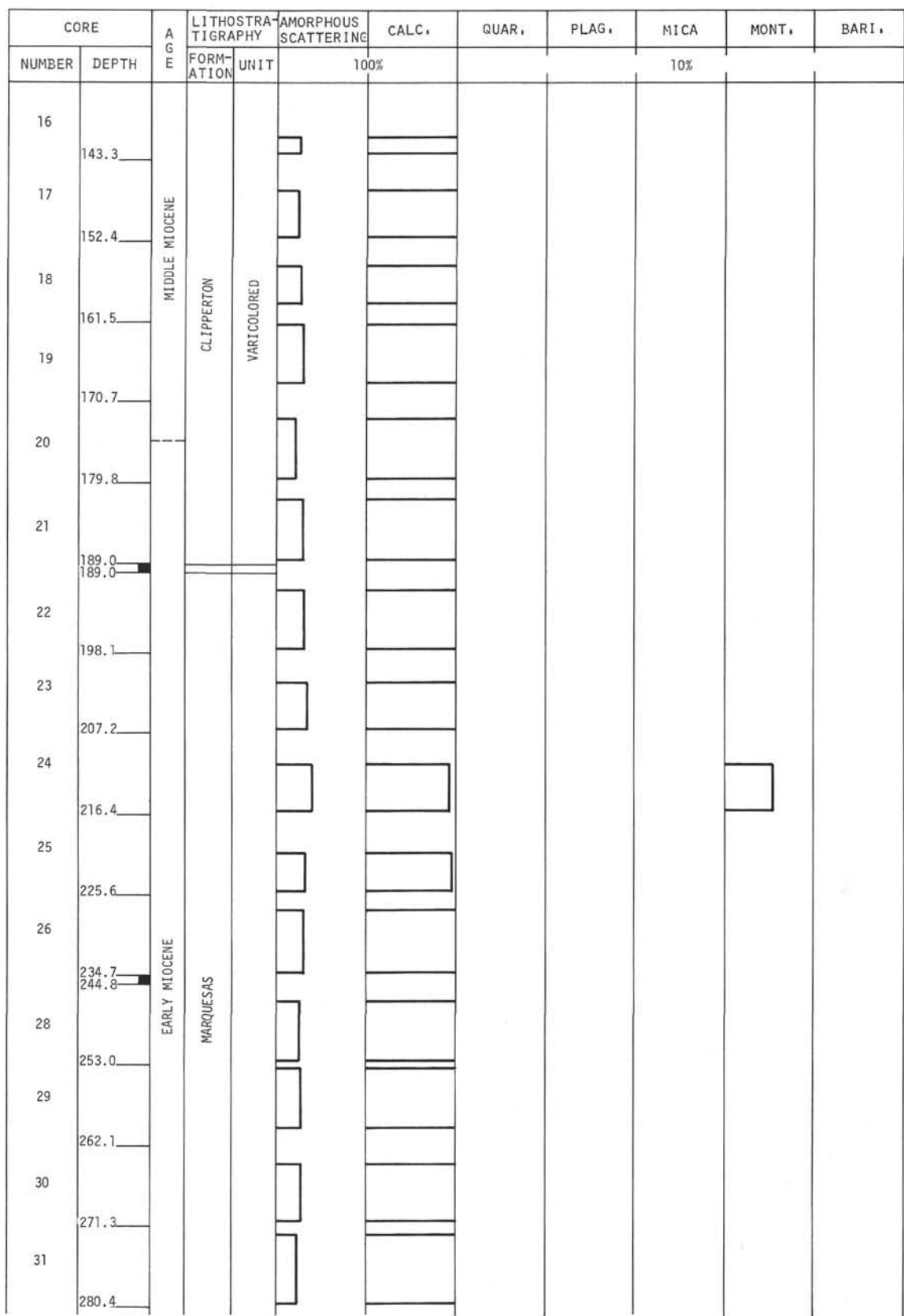


Figure 13. *Continued.*

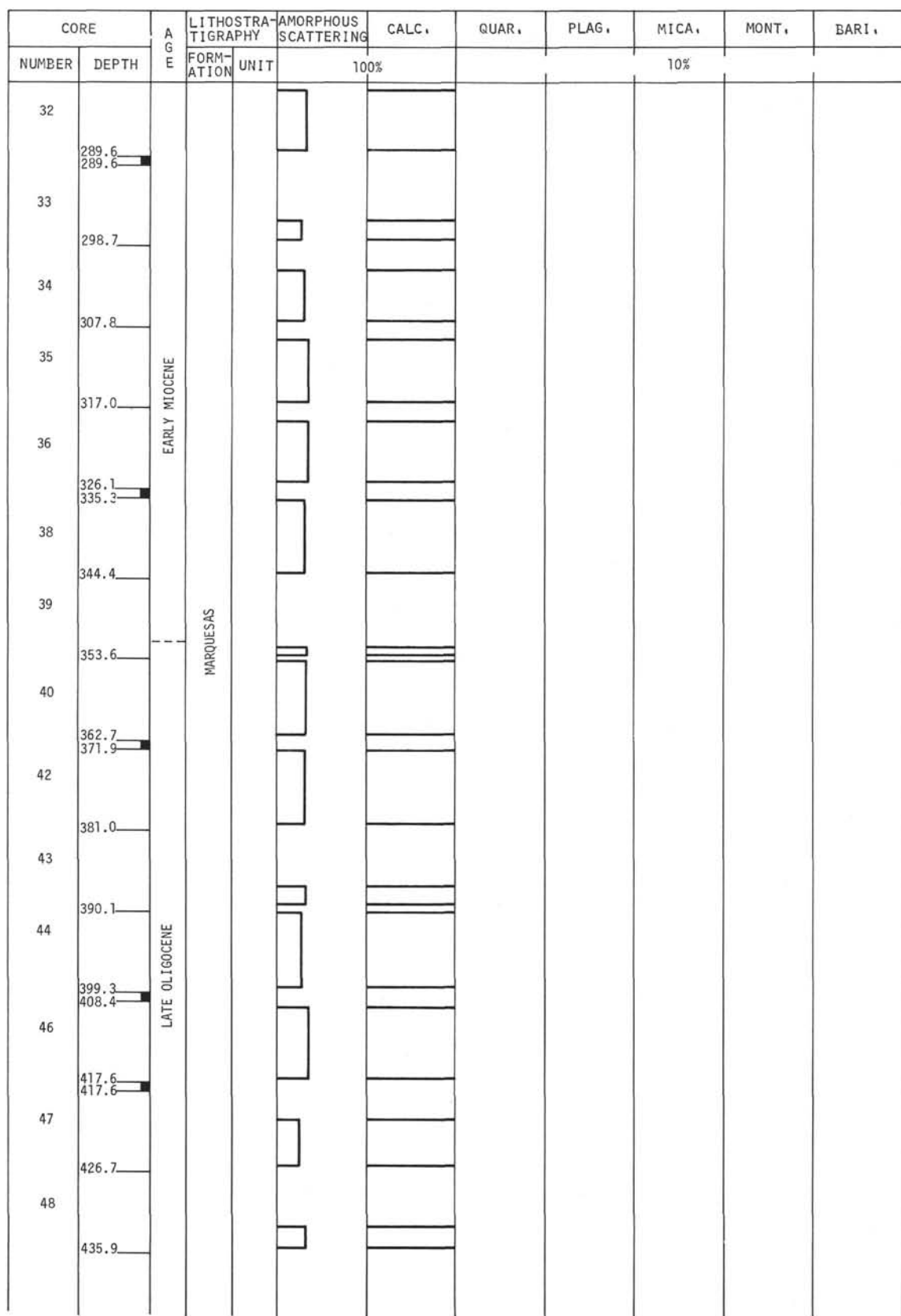


Figure 13. *Continued.*

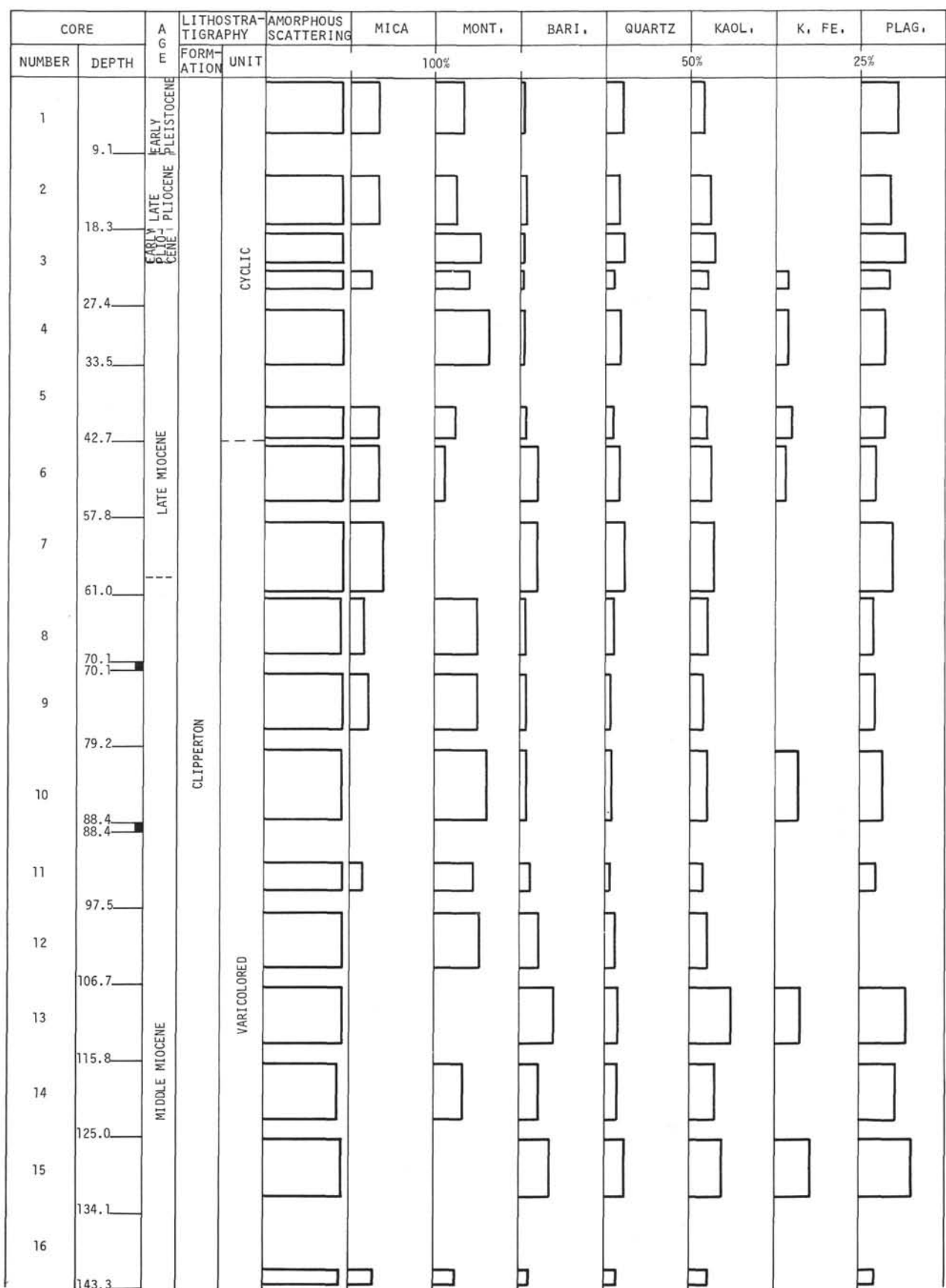


Figure 14. Site 71. Less than  $2\mu$ .

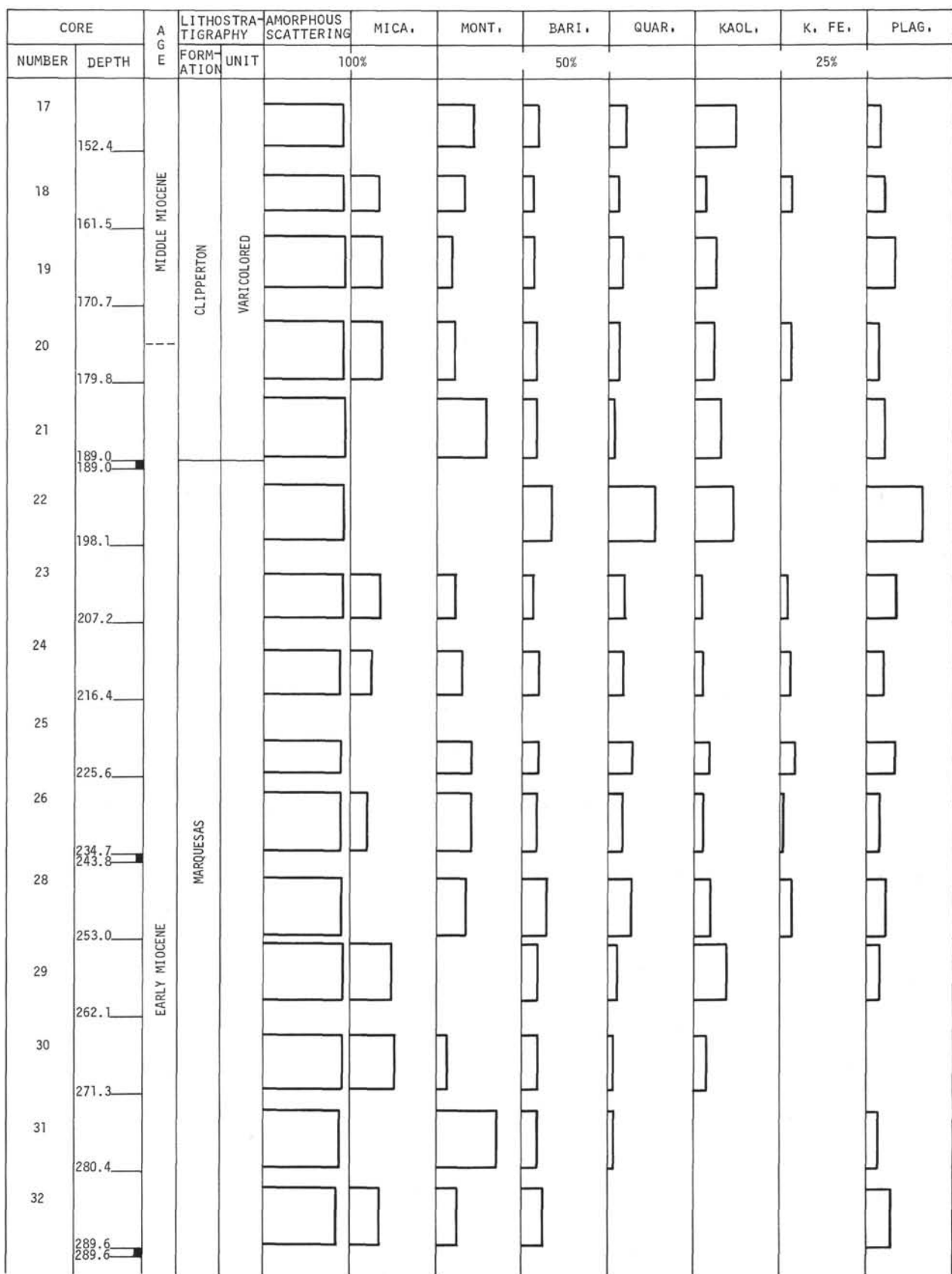


Figure 14. *Continued.*

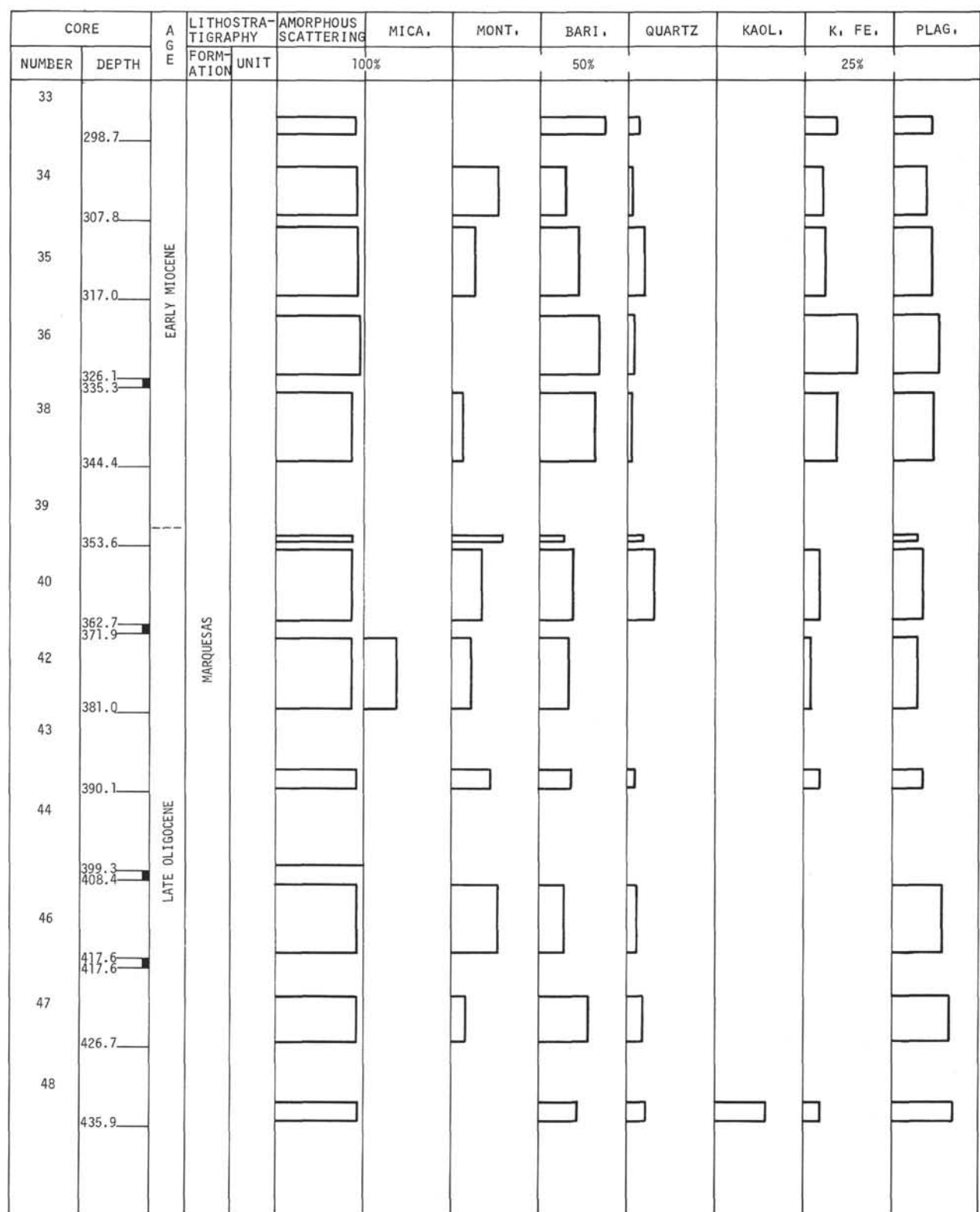


Figure 14. *Continued.*

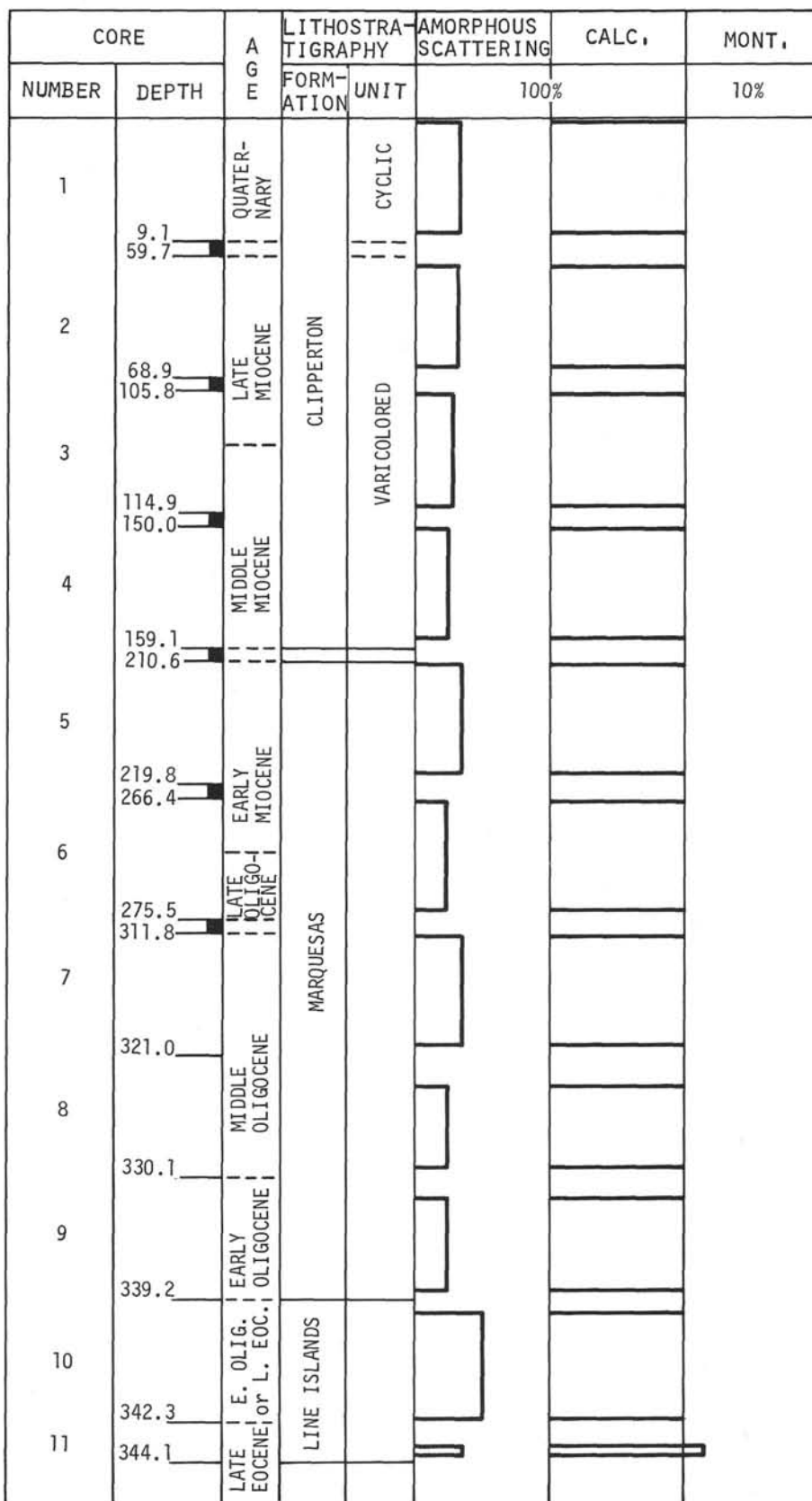


Figure 15. Site 72. Bulk.

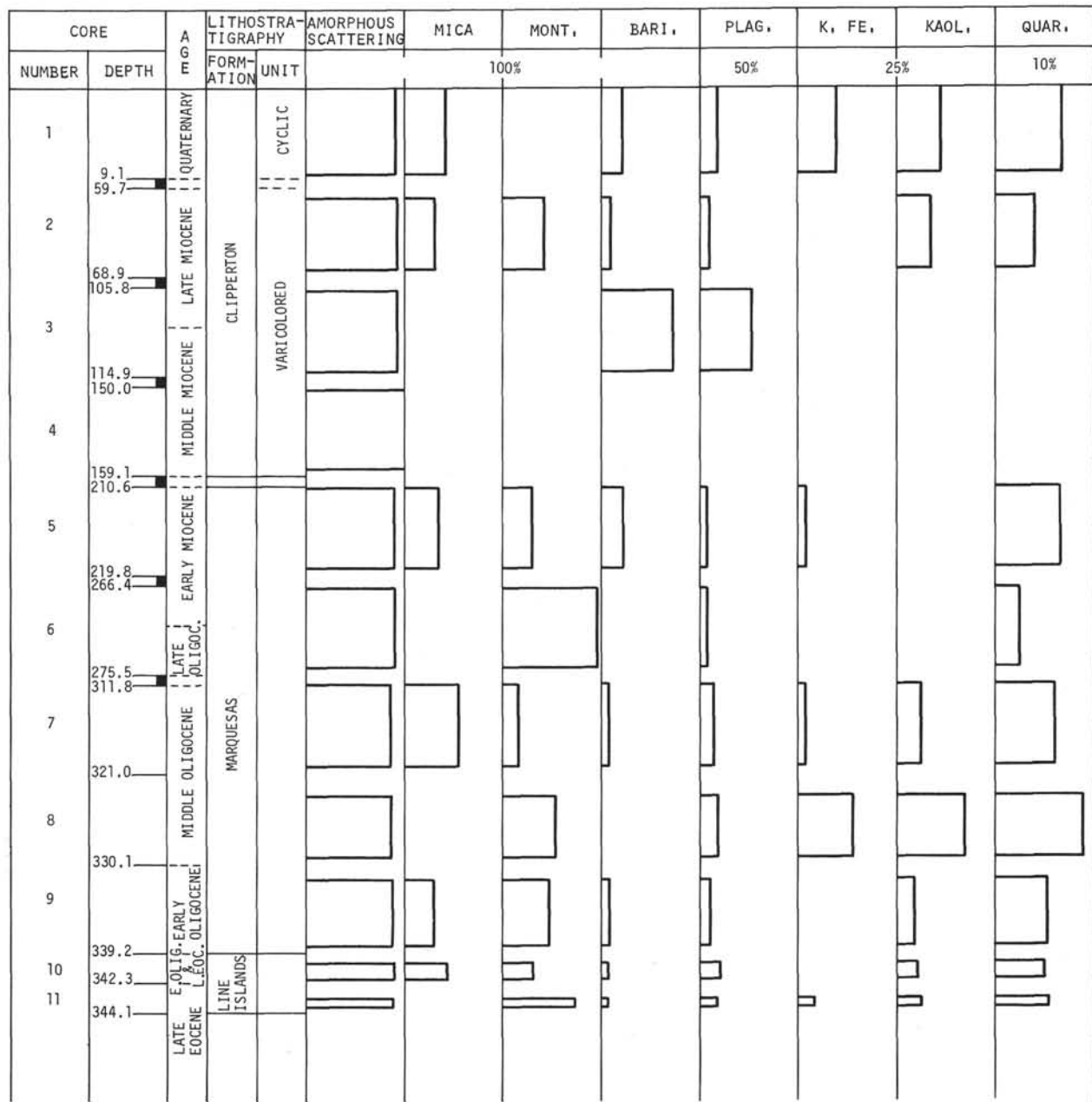


Figure 16. Site 72. Less than  $2\mu$ .

amorphous material was diluted by an influx of calcareous material at sites closest to the equatorial high productivity belt. However, this or other explanations depend on interpretations of the latitudinal positions of these sites during the Miocene and Pliocene times in the framework of sea floor spreading.

The varicolored unit of the Clipperton Formation is consistently highly calcareous and, in this respect, differs from the other units of the formation. Its characteristic pastel shades of purple, blue and green may be due to minute amounts of amorphous manganese oxides and amorphous iron in a reduced state.

In general, the Marquesas Oceanic Formation is also consistently highly calcareous like the overlying varicolored unit of the Clipperton. However, the Marquesas tends to be a relatively massive formation, very light gray to light bluish-white in color. If the pastel colors in the Clipperton are due to amorphous manganese and iron constituents the Marquesas may have only trace amounts of these materials.

The Line Islands Oceanic Formation is characterized by its moderately high amorphous scattering percentage and a brown color. Both of these parameters appear to be largely due to the high content of

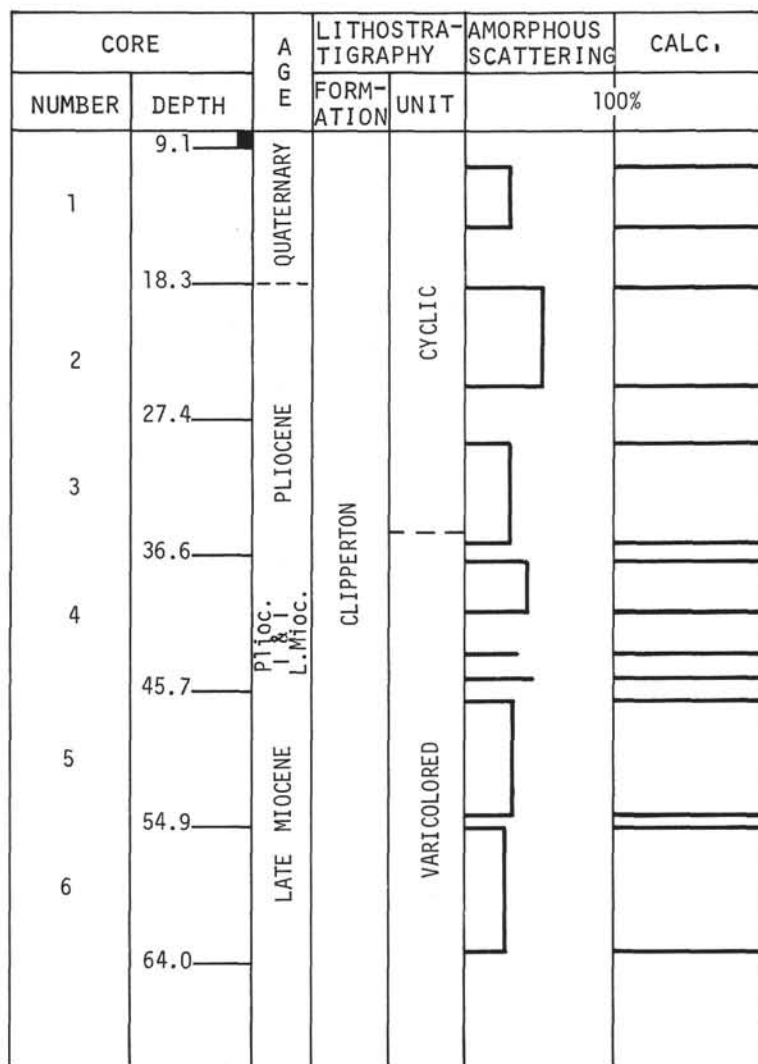


Figure 17. Site 72A. Bulk.

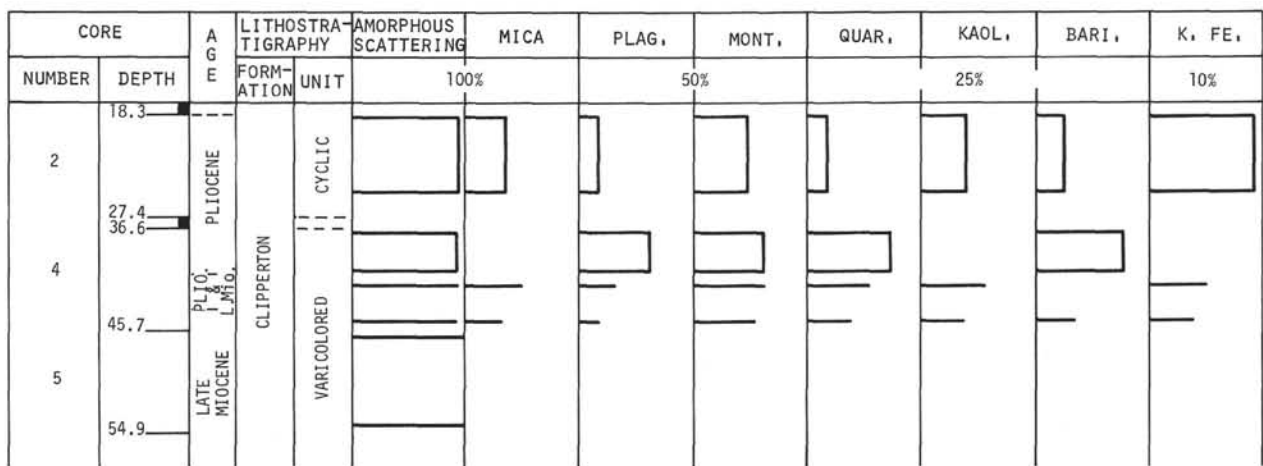


Figure 18. Site 72A. Less than 2 $\mu$ .

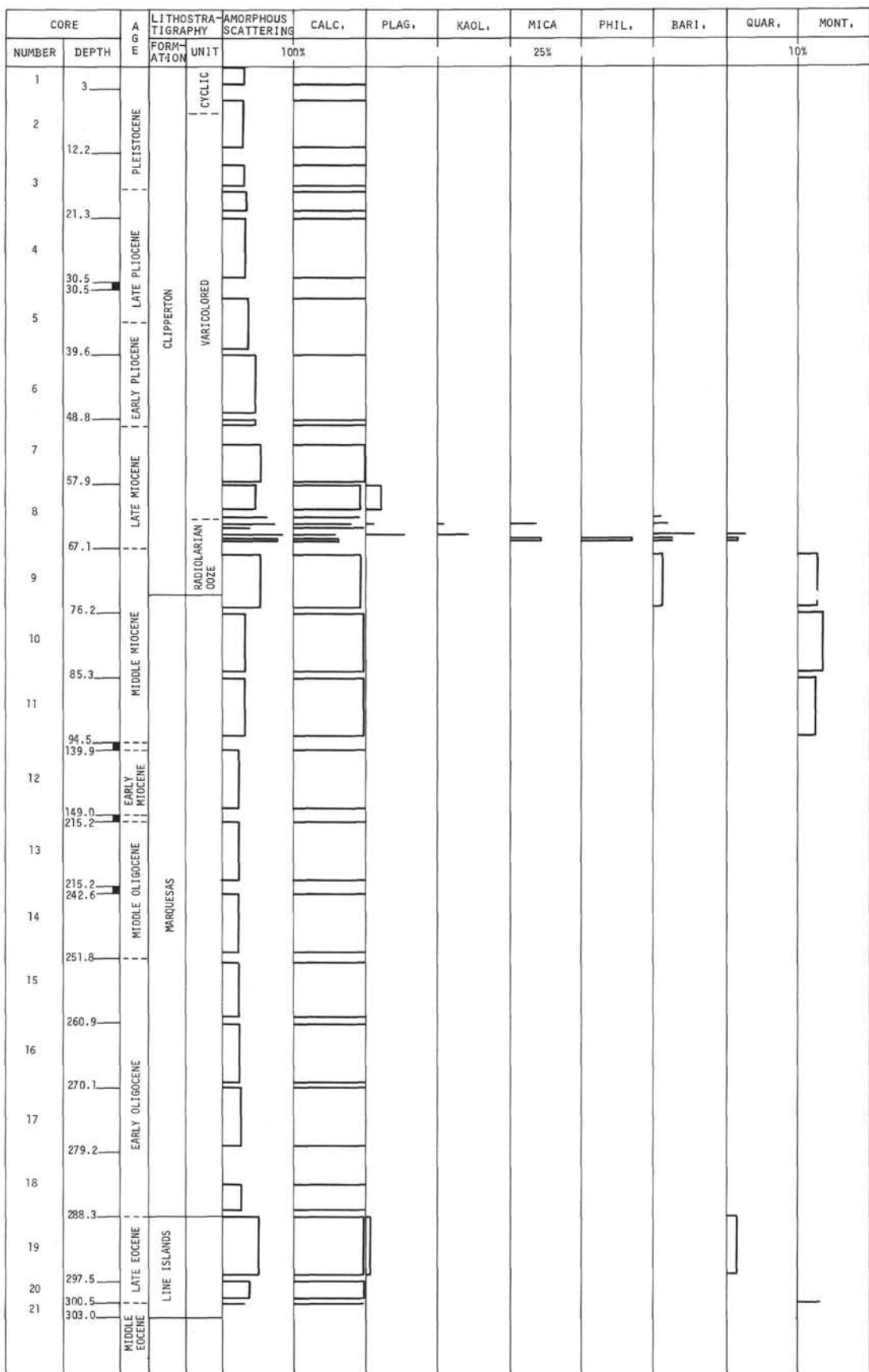


Figure 19. Site 73. Bulk.

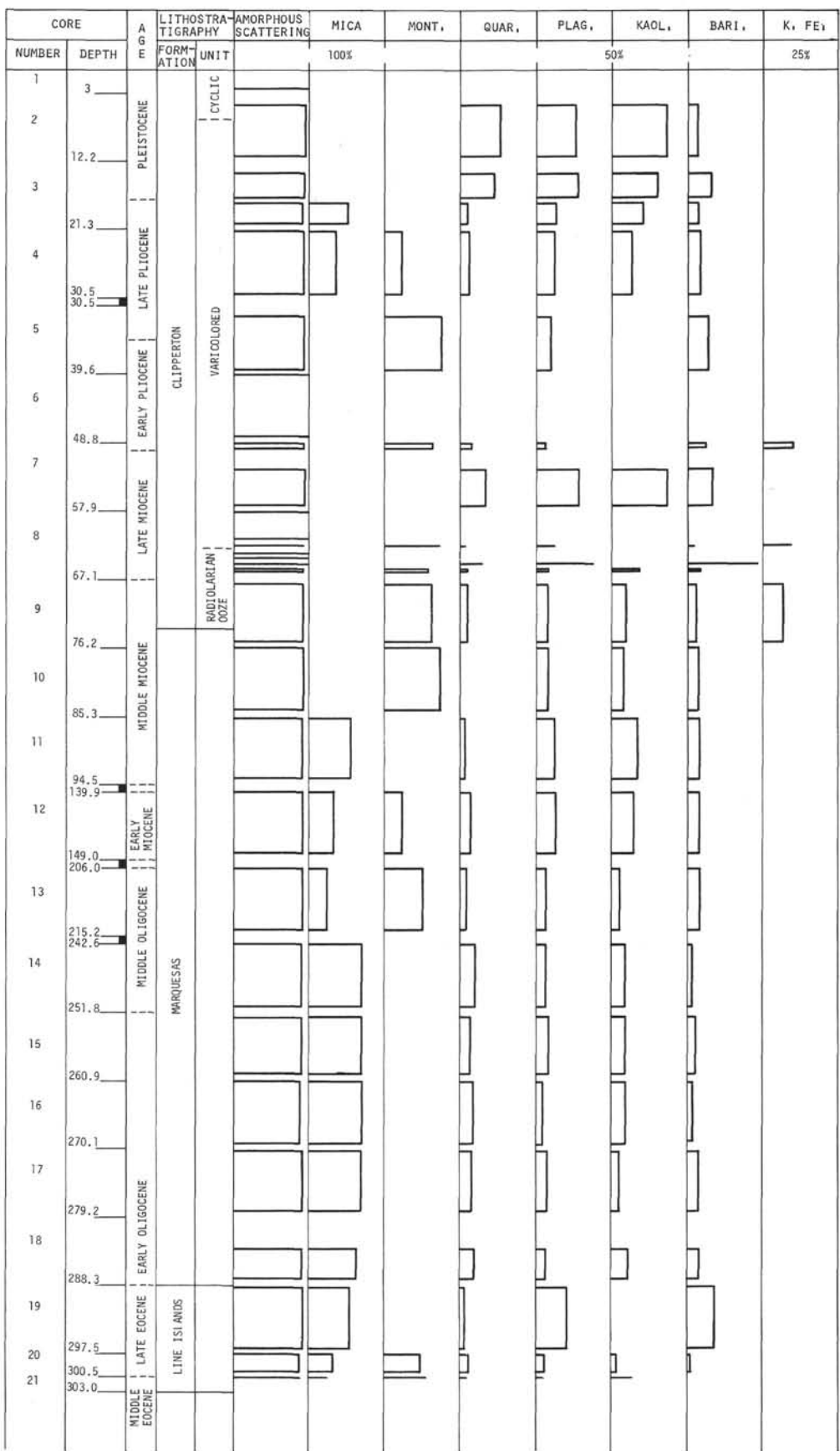


Figure 20. Site 73. Less than 2 $\mu$ .

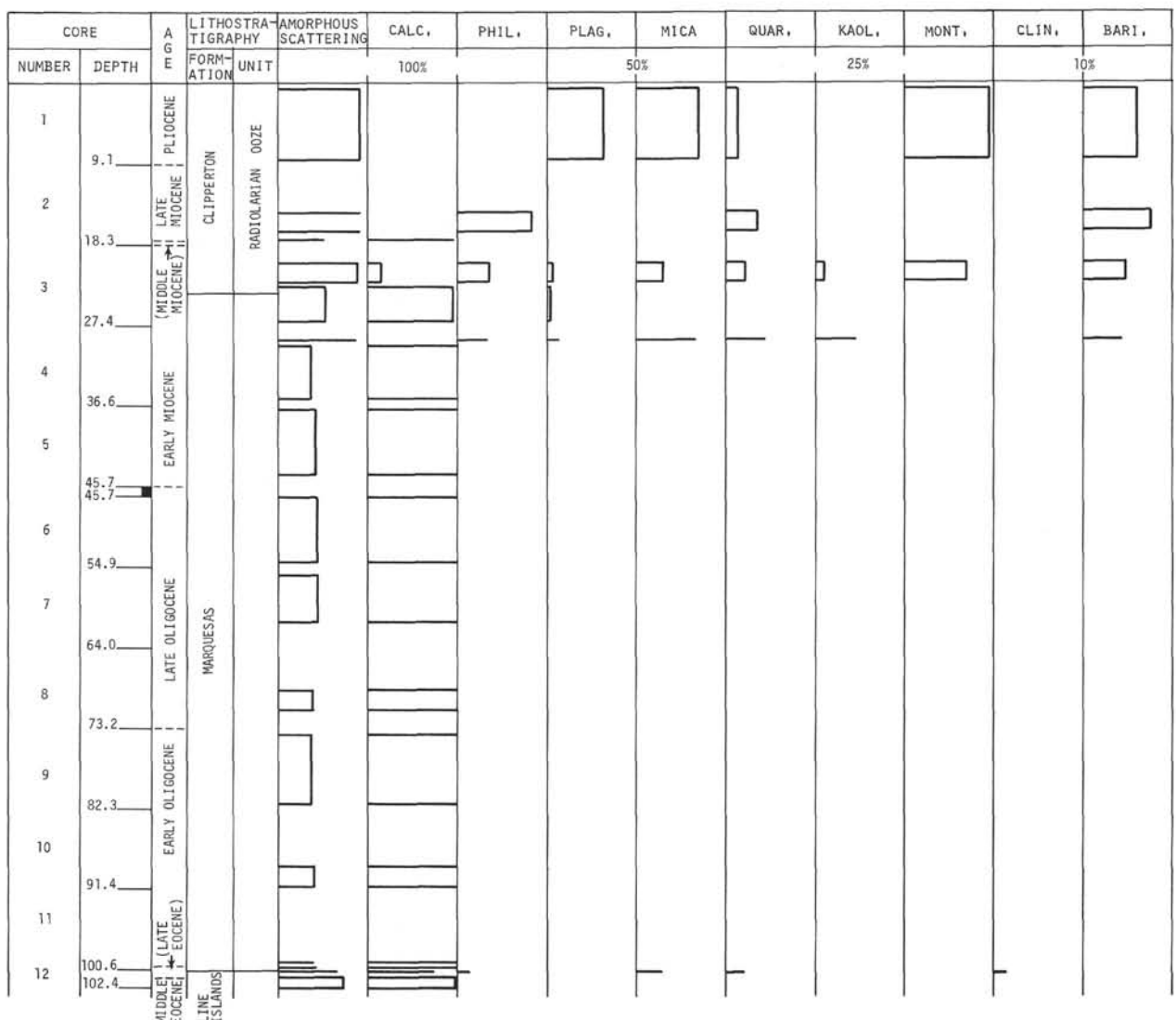


Figure 21. Site 74. Bulk.

amorphous iron and manganese oxides. Goethite was found at Sites 74 and 75. The occurrence of this facies above basaltic basement as at Site 74 further substantiates the suggestion (Bostrom and Peterson, 1966, 1969) that during the formation of new basaltic basement at sea-floor spreading centers exhalations of iron- and manganese-rich solutions probably occur.

Both the zeolites phillipsite and clinoptilolite occur in Leg 8 cores; however, phillipsite has a much wider stratigraphic and geographic distribution than clinoptilolite. Clinoptilolite is found only at Site 74 in the Late Eocene Line Islands Formation and at Site 68 in an unnamed, Middle Eocene unit. At both sites it occurs with phillipsite. In contrast, phillipsite is found at five sites. It occurs most abundantly in the radio-

larian ooze unit of the Clipperton Formation (Sites 70, 73 and 74). At Sites 73 and 74 it occurs in Miocene radiolarian oozes, and at Site 70 in Pliocene radiolarian oozes. In addition, phillipsite is found in the Late Eocene Line Islands Formation and Early Miocene Marquesas Formation at Site 74, Oligocene Marquesas Formation at Site 75, Quaternary residuum at Site 75, and unnamed Eocene sediments at Site 68. Occasional occurrences of volcanic glass and ashy layers were reported by the shipboard scientists at these sites. This suggests a probable authigenic origin for the zeolites, with the volcanic glass supplying the necessary cations and silica.

The almost ubiquitous occurrence of barite is puzzling. As discussed above, this barite does not seem to

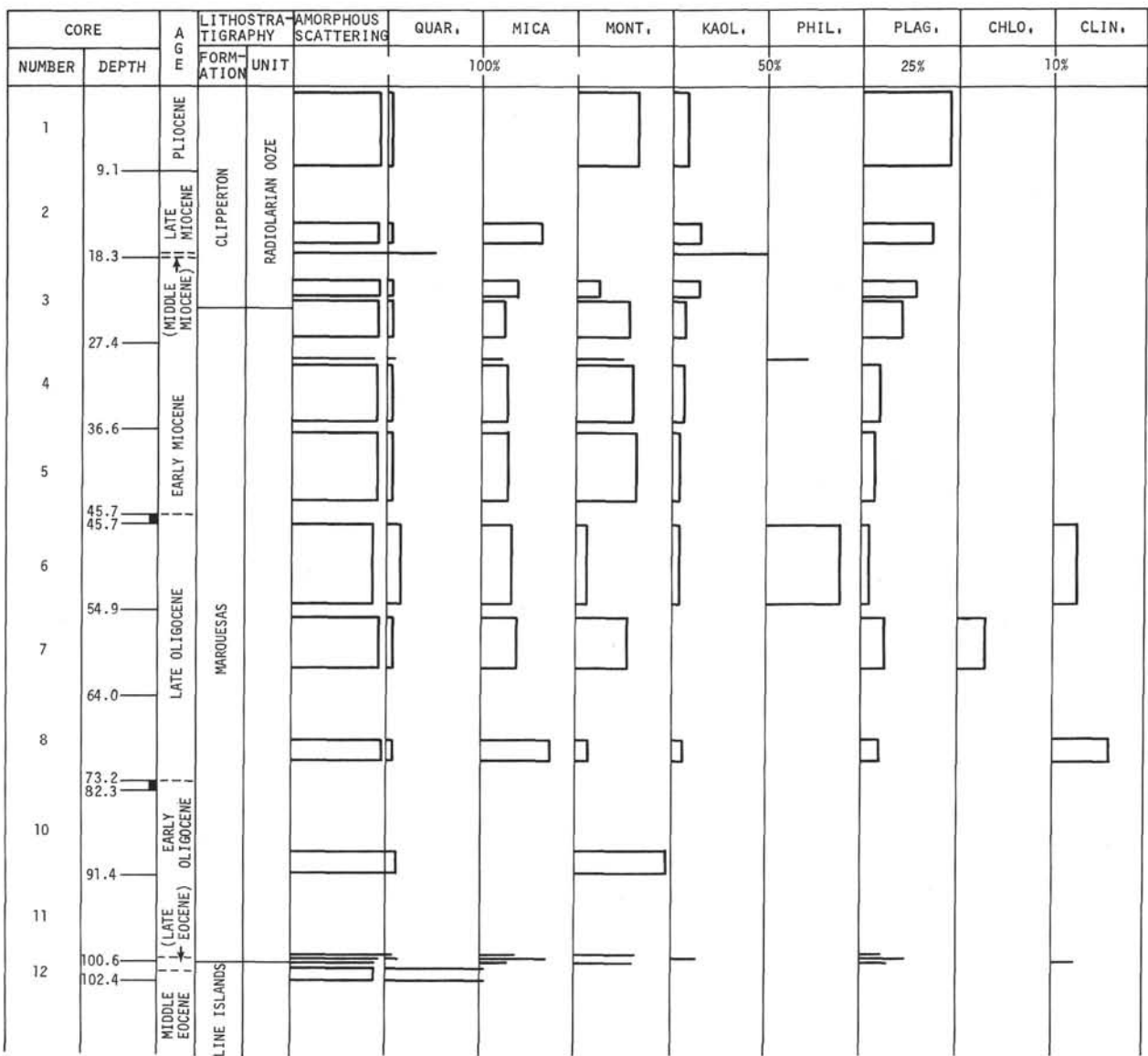


Figure 22. Site 74. Less than 2 $\mu$ .

represent contamination by drilling muds. It is found in trace amounts in virtually all decalcified silt-size and less than 2-micron fractions. There is, however, an apparent correlation between barite content and stratigraphic position when one looks at the results from the bulk analyses. In the bulk analyses, with one exception (Site 74), barite is only found in the radiolarian ooze units of the Clipperton Formation at Sites 70, 73 and 74 (Figures 7, 19 and 21) and in the Line Islands Formation of Sites 69, 70 and 74 (Figures 3, 5, 9 and 21). These stratigraphic units are the ones which contain varying amounts of amorphous iron-manganese oxides. In addition, at Sites 70, 73 and 74 each occurrence of phillipsite in the radiolarian ooze unit of

the Clipperton Formation was accompanied by the presence of barite (Figures 7, 19 and 21). The barite is probably authigenic, but whether or not there is a genetic relationship between barite, iron-rich sediments and phillipsite is not known at this time.

In the decalcified silt and clay fractions, the highest frequencies of barite occurrence are seen at Sites 70, 71, 72 and 73, the sites closest to the equator. This distribution suggests that the occurrence of barite is related to the equatorial zone of high organic productivity. Barite may form authigenically at low temperatures from the traces of barium in organic matter.

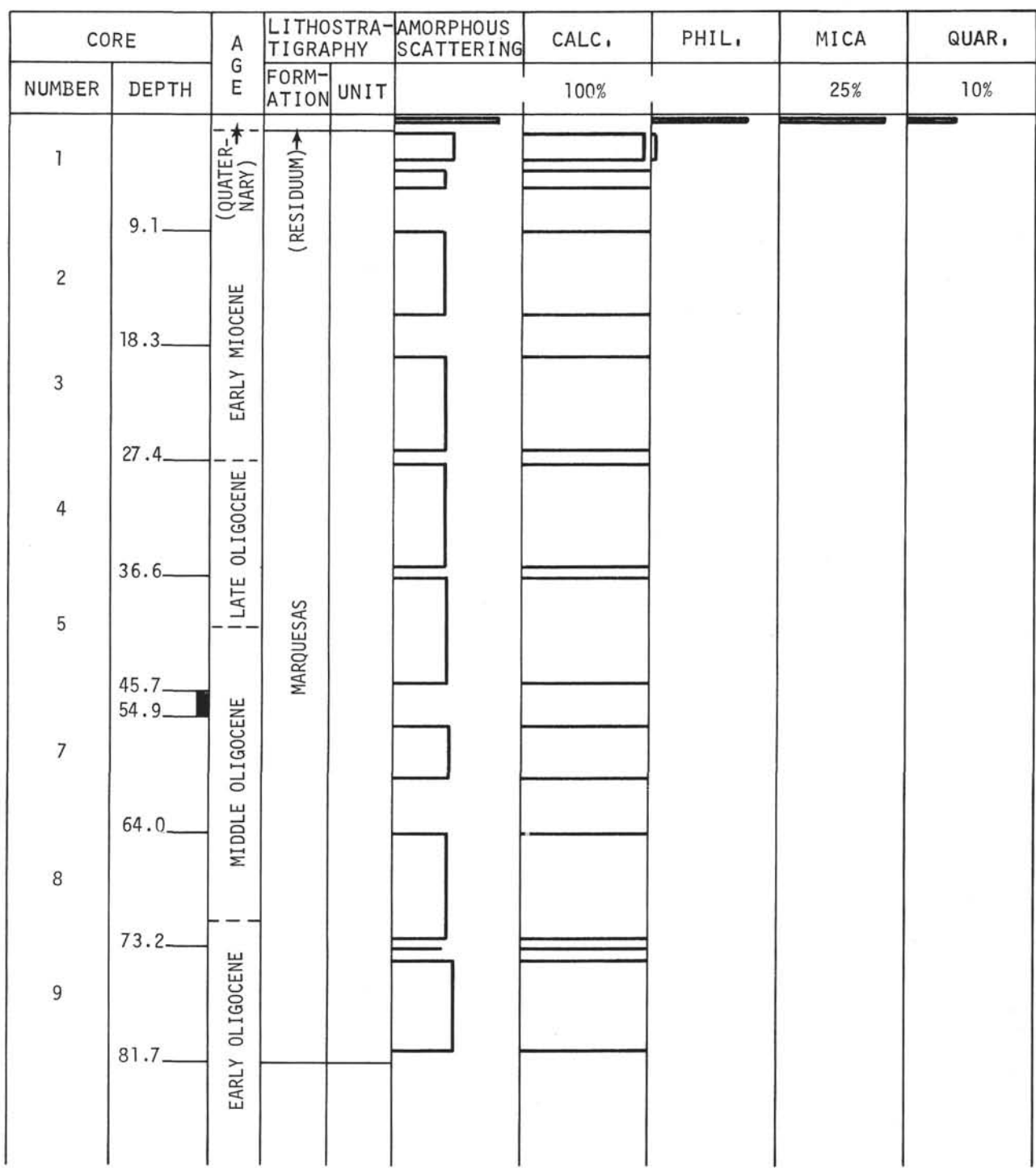


Figure 23. Site 75. Bulk.

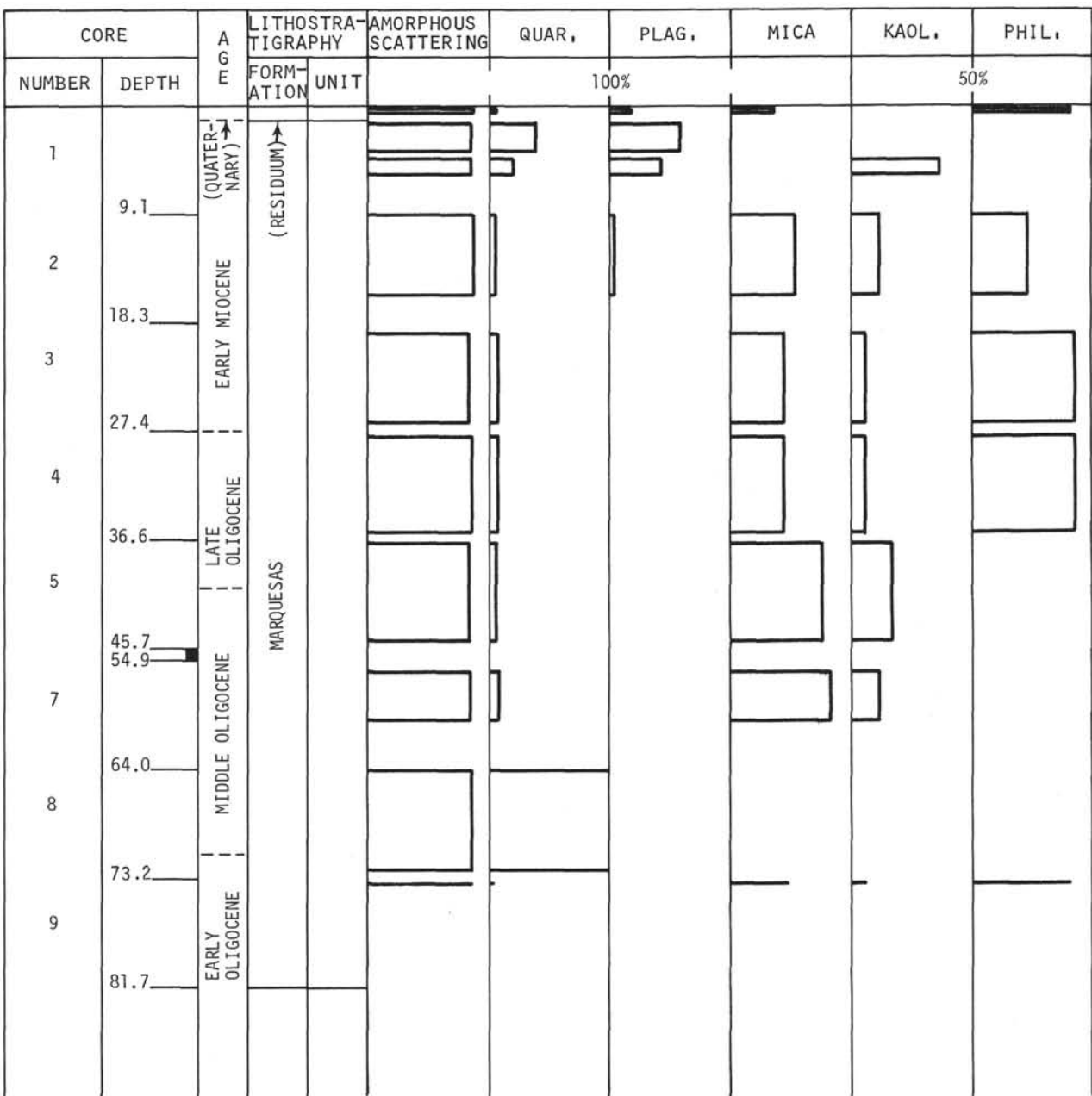


Figure 24. Site 75. Less than  $2\mu$ .

More detailed sampling and petrologic work, and a good idea of the latitudinal position of these sites through time are necessary to confirm or modify these hypotheses and to arrive at a better understanding of the origin of barite in deep-sea environments.

#### REFERENCES

Bostrom, K. and Peterson, M. N. A., 1966. Precipitates from hydrothermal exhalations on the East Pacific Rise. *Econ. Geol.* 61, 1258.

\_\_\_\_\_, 1969. The origin of aluminum-poor ferromanganese sediments in areas of high heat flow on the East Pacific Rise. *Marine Geol.* 7, 427.

Rex, R. W., et al., 1971. X-ray mineralogy studies — Leg 6. In Fischer, A. G., et al., 1971, *Initial Reports of the Deep Sea Drilling Project, Volume VI*. Washington (U. S. Government Printing Office), 691.

**TABLE 1**  
**Results of X-Ray Diffraction Analysis from Site 68**

**Hole 68: Bulk**

Core	Depth	Sample Depth Below Sea Floor (m)	Diff.	Amorph.	Quar.	Plag.	Kaol.	Mica	Mont.	Clin.	Phil.
1	0-7.6	0.10-6.62	81.5	71.1	5.4	6.3	14.2	6.7	14.1	11.1	42.2
2	7.6-14.9	8.10-14.35	80.2	69.1	5.2	6.5	15.4	9.3	8.4	13.3	41.9

**Hole 68: 2-20 $\mu$**

Core	Depth	Sample Depth Below Sea Floor (m)	Lithostratigraphy			
			Formation	Unit	Amorph.	Clin.
1	0-7.6	0.10-6.62			64	P M
2	7.6-14.9	8.10-14.35		Not Determined	74	P M

**Hole 68: < 2 $\mu$**

Core	Depth	Sample Depth Below Sea Floor (m)	Diff.	Amorph.	Quar.	Plag.	Kaol.	Mica	Mont.	Clin.	Phil.
1	0-7.6	0.10-6.62	92.3	88.0	6.6	6.9	6.5	30.0	26.5	5.2	18.3
2	7.6-14.9	8.10-14.35	93.0	89.1	5.5	16.8	14.5	38.5	13.2	11.5	-

**TABLE 2**  
**Results of X-Ray Diffraction Analysis from Site 69**

**Hole 69: Bulk**

Core	Depth	Sample Depth Below Sea Floor (m)	Diff.	Amorph.	Calc.	Quar.	K-Fe.	Plag.	Kaol.	Mica	Bari.
2	14.3-23.5	14.46-22.67	86.5	79.0	75.0	6.1	6.5	5.4	7.0	—	—
3	23.5-32.6	23.60-30.32	86.7	79.3	59.7	5.6	4.3	6.0	5.6	18.8	—
		31.14-31.72	61.2	39.4	100.0	—	—	—	—	—	—
4	52.1-61.3	52.24-58.42	63.2	42.5	100.0	—	—	—	—	—	—
5	116.4-125.6	116.47-124.60	68.3	50.5	99.4	—	—	—	—	—	—
6	186.5-195.7	182.62-194.82	93.9	90.5	—	—	—	—	—	—	100.0

**Hole 69: 2-20 $\mu$**

Core	Depth	Sample Depth Below Sea Floor (m)	Lithostratigraphy				Amorph.	Bari.
			Formation	Unit				
2	14.3-23.5	14.46-22.62		Radiolarian ooze			94	M
3	23.5-32.6	23.60-30.32	Clipperton	Cyclic			96	M
		31.14-31.72					97	M
4	52.1-61.3	52.24-58.42	Marquesas				88	M
5	116.4-125.6	116.47-124.60					88	M
6	186.5-195.7	182.62-194.82	Line Islands				99	M

**Hole 69: < 2 $\mu$**

Core	Depth	Sample Depth Below Sea Floor (m)	Diff.	Amorph.	Quar.	K-Fe.	Plag.	Kaol.	Mica	Mont.	Bari.
2	14.3-23.5	14.46-22.67	97.8	96.5	10.9	—	11.7	18.9	27.5	30.9	—
3	23.5-32.6	23.60-30.32	92.8	88.8	13.3	10.0	16.5	12.5	27.3	15.0	5.3
		31.14-31.72	94.2	90.9	14.6	10.0	17.4	18.4	26.4	13.2	—
4	52.1-61.3	52.24-58.42	93.6	90.0	7.5	4.7	15.8	14.1	57.9	—	—
5	116.4-125.6	116.47-124.60	94.7	91.7	8.3	—	18.7	15.5	—	41.2	16.3
6	186.5-195.7	182.62-194.82	96.9	95.2	14.8	—	25.7	—	59.4	—	—

**Hole 69A: Bulk**

Core	Depth	Sample Depth Below Sea Floor (m)	Diff.	Amorph.	Calc.	Quar.	K-Fe.	Plag.	Mica	Mont.	Bari.
1	61.3-70.4	61.36-69.42	63.7	43.3	98.7	—	—	—	—	—	—
2	70.4-79.6	70.50-78.65	65.3	45.8	98.5	—	—	1.0	—	—	—
3	79.6-88.7	80.31-88.22	59.5	36.7	96.8	—	—	—	—	3.0	—

TABLE 2 – *Continued***Hole 69A: Bulk – *Continued***

Core	Depth	Sample Depth Below Sea Floor (m)	Diff.	Amorph.	Calc.	Quar.	K-Fe.	Plag.	Mica	Mont.	Bari.
4	88.7-99.8	88.80-97.02	55.2	30.0	100.0	—	—	—	—	—	—
5	97.8-107.0	97.89-106.00	57.5	33.6	100.0	—	—	—	—	—	—
6	107.0-116.1	107.44-115.62	59.4	36.6	100.0	—	—	—	—	—	—
7	125.3-134.4	132.70-134.12	65.6	46.3	99.6	—	—	—	—	—	—
8	134.4-143.6	134.55-142.50	62.7	41.7	99.6	—	—	—	—	—	—
9	143.6-152.7	143.64-150.33	91.7	87.1	—	16.7	—	22.4	—	—	60.9
10	152.7-161.8	152.89-160.91	92.2	87.8	—	4.2	—	—	53.4	—	42.4
11	213.7-222.8	213.82-221.94	93.7	90.2	—	—	12.2	12.2	—	49.0	26.6
12	222.8-229.5	223.20	94.7	91.7	—	—	—	—	—	71.1	28.9

**Hole 69A: 2-20μ**

Core	Depth	Sample Depth Below Sea Floor (m)	Lithostratigraphy			
			Formation	Unit	Amorph.	Bari.
1	61.3-70.4	61.36-69.42	Marquesas		92	M
2	70.4-79.6	70.50-78.65			89	M
3	79.6-88.7	80.31-88.22			91	M
4	88.7-97.8	88.80-97.02			92	M
5	97.8-107.0	97.89-106.00			95	M
6	107.0-116.1	107.44-115.6			91	M
7	125.3-134.4	132.70-134.12			91	M
8	134.4-143.6	134.55-142.50			96	M
9	143.6-152.7	143.64-150.33			97	M
10	152.7-161.8	152.89-160.91			96	M
11	213.8-222.8	213.82-221.94			99	M
12	222.8-229.5	223.20			100	—

**Hole 69A: <2μ**

Core	Depth	Sample Depth Below Sea Floor (m)	Diff.	Amorph.	Quar.	Plag.	Kaol.	Mica	Mont.	Bari.
1	61.3-70.4	61.36-69.42	93.9	90.5	5.8	7.6	7.9	25.0	50.1	3.6
2	70.4-79.6	70.50-78.65	94.4	91.3	12.0	24.7	—	—	63.3	—
3	79.6-88.7	80.31-88.22	93.8	90.3	4.6	11.4	11.4	—	62.6	9.9
4	88.7-97.8	88.80-97.02	93.8	90.3	3.0	13.3	9.0	28.3	32.2	14.2
5	98.8-107.0	97.89-106.00	94.4	91.3	2.8	11.4	—	16.2	51.2	18.4
6	107.0-116.1	107.44-115.62	93.8	90.3	5.8	12.8	6.2	—	57.3	18.1

TABLE 2 – *Continued***Hole 69A: < 2 $\mu$  – *Continued***

Core	Depth	Sample Depth Below Sea Floor (m)	Sample Depth Below Sea Floor							
			Diff.	Amorph.	Quar.	Plag.	Kaol.	Mica	Mont.	Bari.
7	125.3-134.4	132.70-134.12	94.4	91.3	3.0	5.8	7.2	20.7	51.4	11.9
8	134.4-143.6	134.55-142.50	94.8	91.9	6.4	9.0	—	34.9	33.4	16.3
9	143.6-152.7	143.64-150.33	95.2	92.9	3.8	5.3	—	28.9	56.5	5.5
10	152.7-161.8	152.89-160.91	94.6	91.6	4.8	4.9	6.8	21.6	56.1	5.7
11	213.8-222.8	213.82-221.94	92.8	88.8	1.0	—	—	8.2	88.6	1.5
12	222.8-229.5	223.20	94.6	91.6	2.1	3.4	—	—	94.5	—

**TABLE 3**  
**Results of X-Ray Diffraction Analysis from Site 70**

**Hole 70: Bulk**

Core	Depth	Sample Depth Below Sea Floor (m)										
			Diff.	Amorph.	Calc.	Quar.	Plag.	Kaol.	Mica	Mont.	Phil.	Bari.
1	0-9.1	0.88-2.18	93.1	89.2	—	12.7	16.0	13.6	52.7	—	—	4.9
		3.22-6.83	65.4	45.9	—	12.6	—	—	20.7	34.8	29.3	2.7
		7.58-8.08	94.4	91.3	—	13.6	23.1	15.4	39.7	—	—	8.3
2	9.1-16.8	14.80-16.13	95.2	92.5	—	8.6	18.9	18.0	37.7	—	—	16.8
3	16.8-25.9	17.10-18.45	95.0	92.2	—	8.6	24.2	17.1	37.0	—	—	13.1
		19.60-25.01	73.9	59.2	99.3	—	—	—	—	—	—	—
4	25.9-35.1	26.03-32.60	76.6	63.5	98.8	1.2	—	—	—	—	—	—
5	35.1-44.2	35.28-43.37	81.0	70.3	97.3	—	—	—	—	—	—	2.4
6	44.2-53.3	44.38-52.22	68.2	50.3	100.3	—	—	—	—	—	—	—
7	53.3-62.5	53.40-61.50	68.7	51.1	100.0	—	—	—	—	—	—	—
8	62.5-71.6	62.61-70.68	63.9	43.6	100.0	—	—	—	—	—	—	—
9	71.6-80.8	77.98	68.7	51.1	100.0	—	—	—	—	—	—	—
10	80.8-89.9	80.85-89.12	63.6	43.1	100.0	—	—	—	—	—	—	—
11	94.8-103.9	101.00-102.60	63.2	42.5	100.0	—	—	—	—	—	—	—
12	103.9-113.1	107.41-112.80	66.9	48.3	100.0	—	—	—	—	—	—	—

**Hole 70: 2-20μ**

Core	Depth	Sample Depth Below Sea Floor (m)	Lithostratigraphy			
			Formation	Unit	Amorph.	Bari.
1	0-9.1	0.88-2.18	Clipperton	Radiolarian Ooze	98	—
		3.22-6.83			89	P
		7.58-8.08			93	P
2	9.1-16.8	14.80-16.13	Marquesas	Cyclic	98	P
3	16.8-25.9	17.10-18.45			97	M
		19.60-25.01			98	M
5	35.1-44.2	35.28-43.37			94	M
6	44.2-53.3	44.38-52.22			96	M
7	53.3-62.5	53.40-61.50			91	M
8	62.5-71.6	62.61-70.68			91	M
9	71.6-80.8	77.98			99	—
10	80.8-89.9	80.85-89.12			92	M
11	94.8-103.9	101.00-102.60			99	M
12	103.9-113.1	107.41-112.80			92	M

TABLE 3 – *Continued***Hole 70: < 2 $\mu$** 

Core	Depth	Sample Depth Below Sea Floor (m)										
			Diff.	Amorph.	Quar.	K-Fe.	Plag.	Kaol.	Mica	Chlo.	Mont.	Bari.
1	0.9-1.1	0.88-2.18	93.1	89.2	18.3	—	17.0	7.4	51.8	5.6	—	—
		3.22-6.83	94.6	91.6	12.7	—	15.2	6.8	40.0	3.4	21.8	—
		7.58-8.08	94.4	91.3	12.3	—	17.9	14.8	38.8	—	16.2	—
2	9.1-16.8	14.80-16.13	94.8	91.9	17.3	—	19.1	5.0	41.8	6.3	10.6	—
3	16.8-25.9	17.10-18.45	95.4	92.8	17.3	—	20.9	9.1	43.0	9.7	—	—
		19.60-25.01	94.6	91.6	16.4	—	20.7	24.6	—	—	26.9	11.5
4	25.9-35.1	26.03-32.60	93.5	89.9	14.3	—	16.4	17.1	28.8	—	23.4	—
5	35.1-44.2	35.28-43.37	94.1	90.8	10.2	—	11.7	15.3	57.7	—	—	5.1
6	44.2-53.3	44.38-52.22	94.3	91.1	2.8	—	12.9	14.9	39.2	—	17.8	12.4
7	53.3-62.5	53.40-61.50	95.4	92.8	3.2	25.5	18.2	21.4	—	—	—	31.7
8	62.5-71.6	62.61-70.68	94.4	91.3	4.4	8.9	9.4	10.7	25.6	—	20.8	20.3
9	71.6-80.8	77.98	95.1	92.4	7.0	8.0	12.9	9.4	52.9	—	—	9.8
10	80.8-89.9	80.85-89.12	94.5	91.4	4.8	—	—	47.0	—	—	—	48.2
11	94.8-103.9	101.00-102.60	94.6	91.6	2.3	24.3	16.4	—	—	—	—	57.0
12	103.9-113.1	107.41-112.80	93.5	89.9	2.2	21.2	22.4	—	—	—	—	54.2

**Hole 70A: Bulk**

Core	Depth	Sample Depth Below Sea Floor (m)								
			Diff.	Amorph.	Calc.	Quar.	Cris.	Plag.	Mont.	Bari.
1	113.1-122.2	114.80-121.30	58.0	34.4	100.0	—	—	—	—	—
2	122.2-131.4	122.30-130.38	60.7	38.6	99.6	—	—	—	—	—
4	140.5-149.7	143.00-148.80	58.5	35.2	100.0	—	—	—	—	—
5	149.7-158.8	157.32-158.02	57.0	32.8	100.0	—	—	—	—	—
6	158.8-167.9	159.60-167.12	53.6	27.5	100.0	—	—	—	—	—
7	167.9-177.1	174.02-176.22	55.4	30.3	97.0	—	—	—	3.0	—
8	177.1-186.2	178.70-185.42	52.7	26.1	100.0	—	—	—	—	—
9	186.2-192.3	187.79-191.30	51.3	23.9	100.0	—	—	—	—	—
10	192.3-201.5	195.01-200.40	50.9	23.3	100.0	—	—	—	—	—
11	201.5-210.6	204.56-209.82	52.2	25.3	100.0	—	—	—	—	—
12	210.6-219.8	213.70-218.89	51.6	24.4	100.0	—	—	—	—	—
13	219.8-228.9	224.43-228.00	51.7	24.5	100.0	—	—	—	—	—
14	228.9-238.0	235.00-237.22	54.7	29.2	100.0	—	—	—	—	—
15	238.0-247.2	241.90-246.50	58.9	35.8	100.0	—	—	—	—	—
16	247.2-256.3	252.80-255.40	52.0	25.0	100.0	—	—	—	—	—
17	256.3-262.4	257.50-261.62	55.1	29.9	100.0	—	—	—	—	—
18	262.4-268.5	265.50-267.72	52.4	25.6	100.0	—	—	—	—	—

TABLE 3 – *Continued***Hole 70A: Bulk – *Continued***

Core	Depth	Sample Depth Below Sea Floor (m)	Sample Depth Below Sea Floor							
			Diff.	Amorph.	Calc.	Quar.	Cris.	Plag.	Mont.	Bari.
19	268.5-274.6	271.20-273.82	57.2	33.1	99.7	—	—	—	—	—
21	280.7-286.8	286.18	62.2	41.0	99.7	—	—	—	—	—
22	286.8-292.9	289.90-292.12	57.1	33.0	100.0	—	—	—	—	—
23	292.9-299.0	296.60-298.22	58.0	34.4	100.0	—	—	—	—	—
24	299.0-305.1	301.40-304.32	58.2	34.7	99.7	—	—	—	—	—
25	305.1-311.2	308.20-310.92	59.4	36.6	100.0	—	—	—	—	—
27	320.3-326.4	323.00-323.40	58.0	34.4	100.0	—	—	—	—	—
		324.62-325.65	57.6	33.8	99.7	—	—	—	—	—
28	326.4-328.3	327.00-327.65	91.1	86.1	—	5.4	—	19.3	38.1	37.2
30	329.5-331.0	330.89	91.6	86.9	—	—	96.9	—	—	3.1

**Hole 70A: 2-20μ**

Core	Depth	Sample Depth Below Sea Floor (m)	Lithostratigraphy			
			Formation	Unit	Amorph.	Bari.
1	113.1-122.2	114.80-121.30			88	M
4	140.5-149.7	143.00-148.80			91	M
5	149.7-158.8	157.32-158.02			93	M
6	158.8-167.9	159.60-167.12			85	M
7	167.9-177.1	174.02-176.22			86	M
8	177.1-186.2	178.70-185.42			84	M
9	186.2-192.3	187.79-191.30			95	M
10	192.3-201.5	195.01-200.40			90	M
11	201.5-210.6	204.56-209.82	MARQUESAS		90	M
12	210.6-219.8	213.70-218.90			92	M
13	219.8-228.9	224.43-228.00			92	M
14	228.9-238.0	235.00-237.22			91	M
15	238.0-247.2	241.90-246.50			90	M
16	247.2-256.3	252.80-255.40			88	M
17	256.3-262.4	257.50-261.62			90	M
18	262.4-268.5	265.50-267.72			87	M
19	268.5-274.6	271.20-273.82			94	M
21	280.7-286.8	286.18			95	M
22	286.8-292.9	289.90-292.12			91	M
23	292.9-299.0	296.60-298.22			92	M
24	299.0-305.1	301.40-304.32			97	M
25	305.1-311.2	308.20-310.92			93	M

TABLE 3 – *Continued***Hole 70A: 2-20 $\mu$  – *Continued***

Core	Depth	Sample Depth Below Sea Floor (m)	Lithostratigraphy			
			Formation	Unit	Amorph.	Bari.
27	320.3-326.4	323.00-323.42	Line Islands		97	M
		324.62-325.65			92	M
28	326.4-328.3	327.00-327.65			93	M
30	329.5-331.0	330.89			99	M

**Hole 70A: < 2 $\mu$** 

Core	Depth	Sample Depth Below Sea Floor (m)	Chemical Compositions (%)									
			Diff.	Amorph.	Quar.	Cris.	K-Fe.	Plag.	Kaol.	Mica	Mont.	Bari.
1	113.1-122.2	114.80-121.30	93.3	89.6	9.8	—	—	9.8	8.1	23.2	31.4	17.8
2	122.2-131.4	122.30-130.38	92.9	88.9	7.7	—	—	11.0	7.7	43.0	—	30.7
4	140.5-149.7	143.00-148.80	93.6	90.0	12.7	—	—	15.3	—	—	46.5	25.4
5	149.7-158.8	157.32-158.02	94.5	91.4	5.6	—	—	18.9	—	—	44.0	31.5
6	158.8-167.9	159.60-167.12	92.9	88.9	4.8	—	—	13.3	—	—	64.2	17.7
7	167.9-177.1	174.02-176.22	92.9	88.9	3.3	—	—	6.3	4.0	—	76.4	10.0
8	177.1-186.2	178.70-185.42	93.8	90.3	5.2	—	—	11.3	5.7	—	55.9	22.0
9	186.2-192.3	187.79-191.30	92.9	88.9	3.7	—	—	7.8	6.8	—	63.8	18.0
10	192.3-201.5	195.01-200.40	92.8	88.8	6.3	—	—	14.4	6.0	—	42.7	30.6
11	201.5-210.6	204.56-209.82	93.7	90.2	4.5	—	—	13.0	—	—	24.4	58.2
12	210.6-219.8	213.70-218.90	92.7	88.6	3.5	—	—	13.1	—	—	33.4	50.0
13	219.8-228.9	224.43-228.00	93.6	90.0	3.6	—	—	14.5	—	—	39.7	42.1
14	228.9-238.0	235.00-237.22	93.4	89.7	7.3	—	—	10.4	—	—	62.8	19.5
15	238.0-247.2	241.90-246.50	92.2	87.8	—	—	—	33.2	—	—	—	66.8
16	247.2-256.3	252.80-255.40	90.0	84.4	4.3	—	—	17.1	—	—	59.2	19.4
17	256.3-262.4	257.50-261.62	91.1	86.1	2.0	—	—	5.2	7.4	—	71.6	13.8
18	262.4-268.5	265.50-267.72	93.0	89.1	1.6	—	—	7.2	—	—	77.9	13.3
19	268.5-274.6	271.20-273.82	94.8	91.9	—	—	12.3	9.0	—	25.2	36.8	16.0
21	280.7-286.8	286.18	94.9	92.1	—	—	16.0	9.8	—	50.6	—	22.7
22	286.8-292.9	289.90-292.12	92.9	88.9	3.3	—	—	7.1	—	25.8	56.1	7.7
23	292.9-299.0	296.60-298.22	93.7	90.2	4.7	—	—	8.3	—	—	69.6	17.3
24	299.0-305.1	301.40-304.32	94.3	91.1	2.2	—	11.4	12.3	—	—	54.9	19.1
25	305.1-311.2	308.20-310.92	94.0	90.7	2.9	—	6.7	4.8	—	—	62.8	22.8
27	320.3-326.4	323.00-323.42	93.2	89.4	3.6	—	8.2	5.0	—	—	71.0	12.2
		324.62-325.65	91.8	87.2	5.5	—	—	6.0	—	—	77.8	10.7
28	326.4-328.3	327.00-327.65	93.7	90.2	4.6	—	—	4.3	—	—	76.3	14.9
30	329.5-331.0	330.89	81.6	71.3	2.2	90.1	2.5	—	—	—	3.0	2.2

TABLE 3 – *Continued***Hole 70B: Bulk**

Core	Depth	Sample Depth Below Sea Floor (m)	Diff.	Amorph.	Quar.	Cris.	Bari.
2	384.0-385.6	384.25	81.4	70.9	1.5	91.9	6.6

**Hole 70B: < 2μ**

Core	Depth	Sample Depth Below Sea Floor (m)	Diff.	Amorph.	Cris.	Plag.	Mont.	Bari.
2	384.0-385.6	384.25	82.5	72.7	80.9	1.5	13.5	2.6

**TABLE 4**  
**Results of X-Ray Diffraction Analysis from Site 71**

**Hole 71: Bulk**

Core	Depth	Sample Depth Below Sea Floor (m)	Diff.	Amorph.	Calc.	Quar.	Plag.	Mica	Mont.	Bari.
1	0-9.1	0.35-6.30	64.3	44.2	93.2	1.6	—	3.7	—	—
2	9.1-18.3	11.50-17.20	70.8	54.4	97.4	1.6	1.0	—	—	—
3	18.3-27.4	18.45-22.02	60.3	38.0	99.5	—	—	—	—	—
		23.00-25.02	72.9	57.7	94.0	2.1	1.5	—	—	2.5
4	27.4-33.5	27.60-34.12	61.9	40.5	96.1	—	—	—	3.4	—
5	33.5-42.7	38.21-41.82	57.6	33.8	100.0	—	—	—	—	—
6	42.7-51.8	42.90-49.52	55.7	30.8	99.6	—	—	—	—	—
7	51.8-61.0	52.07-60.12	59.2	36.3	99.7	—	—	—	—	—
8	61.0-70.1	61.14-67.82	60.9	38.9	99.6	—	—	—	—	—
9	70.1-79.2	70.25-76.90	57.5	33.6	99.7	—	—	—	—	—
10	79.2-88.4	79.30-87.50	54.5	28.9	100.0	—	—	—	—	—
11	88.4-97.5	91.60-95.20	56.6	32.2	100.0	—	—	—	—	—
12	97.5-106.7	97.73-104.40	54.6	29.1	100.0	—	—	—	—	—
13	106.7-115.8	106.80-113.50	54.6	29.1	100.0	—	—	—	—	—
14	115.8-125.0	116.00-122.60	55.9	31.1	100.0	—	—	—	—	—
15	125.0-134.1	125.10-131.80	58.9	35.8	99.7	—	—	—	—	—
16	134.1-143.3	140.65-142.28	54.9	29.5	100.0	—	—	—	—	—
17	143.3-152.4	146.60-151.60	53.4	27.2	100.0	—	—	—	—	—
18	152.4-161.5	155.00-159.20	55.5	30.5	100.0	—	—	—	—	—
19	161.5-170.7	162.25-168.30	57.4	33.4	100.0	—	—	—	—	—
20	170.7-179.8	172.40-179.00	51.6	24.4	100.0	—	—	—	—	—
21	179.8-189.0	181.45-188.10	57.1	33.0	100.0	—	—	—	—	—
22	189.0-198.1	190.80-197.30	57.9	34.3	100.0	—	—	—	—	—
23	198.1-207.2	201.20-206.40	60.5	38.3	100.0	—	—	—	—	—
24	207.2-216.4	210.30-215.50	63.1	42.4	94.3	—	—	—	5.3	—
25	216.4-225.6	221.00-224.70	58.9	35.8	99.8	—	—	—	—	—
26	225.6-234.7	227.10-233.90	58.1	34.5	100.0	—	—	—	—	—
28	243.8-253.0	245.40-252.10	55.1	29.9	100.0	—	—	—	—	—
29	253.0-262.1	253.20-259.80	56.5	32.0	100.0	—	—	—	—	—
30	262.1-271.3	263.96-270.40	55.4	30.3	100.0	—	—	—	—	—
31	271.3-280.4	273.02-279.60	53.3	27.0	100.0	—	—	—	—	—
32	280.4-289.1	282.10-288.70	56.2	31.6	100.0	—	—	—	—	—
33	289.6-298.7	295.80-297.80	54.1	28.3	100.0	—	—	—	—	—
34	398.7-307.8	301.45-307.00	55.7	30.8	100.0	—	—	—	—	—
35	307.8-317.0	309.40-316.20	56.8	32.5	100.0	—	—	—	—	—
36	317.0-326.1	318.60-325.30	57.2	33.1	100.0	—	—	—	—	—

TABLE 4 – *Continued***Hole 71: Bulk – *Continued***

Core	Depth	Sample Depth Below Sea Floor (m)	Diff.	Amorph.	Calc.	Quar.	Plag.	Mica	Mont.	Bari.
38	335.3-344.4	335.65-343.60	55.1	29.9	100.0	—	—	—	—	—
39	344.4-353.6	352.10-352.80	57.0	32.8	100.0	—	—	—	—	—
40	353.6-362.7	353.91-361.90	56.5	32.0	100.0	—	—	—	—	—
42	371.9-381.0	372.20-380.20	55.3	30.2	100.0	—	—	—	—	—
43	381.0-390.1	387.13-389.30	56.7	32.4	100.0	—	—	—	—	—
44	390.1-399.3	390.17-398.40	52.3	25.5	100.0	—	—	—	—	—
46	408.4-417.6	408.86-416.75	58.1	34.5	100.0	—	—	—	—	—
47	417.6-426.7	420.70-425.90	51.2	23.8	100.0	—	—	—	—	—
48	426.7-435.9	432.80-435.00	55.3	30.2	100.0	—	—	—	—	—

**Hole 71: 2-20μ**

Core	Depth	Sample Depth Below Sea Floor (m)	Lithostratigraphy			
			Formation	Unit	Amorph.	Clin.
1	0-9.1	0.35-6.30			87	— M
2	9.1-18.3	11.50-17.20			91	— M
3	18.3-27.4	18.45-22.02	CLIPPERTON		99	— M
		23.00-25.02			92	T M
4	27.4-33.5	27.60-34.12			93	T M
5	33.5-42.7	38.21-41.82			83	— M
6	42.7-51.8	42.90-49.52			97	— M
7	51.8-61.0	52.07-60.12			94	— M
8	61.0-70.1	61.14-67.82			94	— M
9	70.1-79.2	70.25-76.90			94	— M
10	79.2-88.4	79.30-87.50			97	— M
11	88.4-97.5	91.60-95.20			92	— M
12	97.5-106.7	97.73-104.40			94	T M
13	106.7-115.8	106.80-113.50			97	T M
14	115.8-125.0	116.00-122.60			95	— M
15	125.0-134.1	125.10-131.80			97	— M
16	134.1-143.3	140.65-142.28			87	— M
17	143.3-152.4	146.60-151.60			91	— M
18	152.4-161.5	155.00-159.20			95	— M
19	161.5-170.7	162.25-168.30			96	— M
20	170.7-179.8	172.40-179.00			94	— M
21	179.8-189.0	181.45-188.10			98	— M
22	189.0-198.1	190.80-197.30			91	— M

TABLE 4 – *Continued*Hole 71: 2-20 $\mu$ 

Core	Depth	Sample Depth Below Sea Floor (m)	Lithostratigraphy			
			Formation	Unit	Amorph.	Clin.
23	198.1-207.2	201.20-206.40	M A R Q U E S A S		94	—
24	207.2-216.4	210.30-215.50			91	—
25	216.4-225.6	221.00-224.70			91	—
26	225.6-234.7	227.10-233.90			91	—
28	243.8-253.0	245.40-252.10			90	—
29	253.0-262.1	253.20-259.80			94	—
30	262.1-271.3	263.96-270.40			89	—
31	271.3-280.4	273.02-279.60			89	—
32	280.4-289.6	282.10-288.70			87	—
33	289.6-298.7	295.80-297.80			93	—
34	298.7-307.8	301.45-307.00			91	—
35	307.8-317.0	309.40-316.20			95	—
36	317.0-326.1	318.60-325.30			95	—
38	335.3-344.4	335.65-343.60			90	—
39	344.4-353.6	352.10-352.80			91	—
40	353.6-362.7	353.91-361.90			96	—
42	371.9-381.0	372.20-380.20			87	—
43	381.0-390.1	387.13-389.30			93	—
44	390.1-399.3	390.17-398.40			91	—
46	408.4-417.6	408.86-416.75			88	—
47	417.6-426.7	420.70-425.90			83	—
48	426.7-435.9	432.80-435.00			86	—

Hole 71: <2 $\mu$ 

Core	Depth	Sample Depth Below Sea Floor (m)	Mineralogy								
			Diff.	Amorph.	Quar.	K-Fe.	Plag.	Kaol.	Mica	Mont.	Bari.
1	0-9.1	0.35-6.30	94.4	91.3	10.2	—	11.4	8.1	33.3	33.8	3.4
2	9.1-18.3	11.50-17.20	95.9	93.6	8.9	—	9.6	11.8	35.7	25.3	8.6
3	18.3-27.4	18.45-22.02	95.7	93.3	11.7	—	13.6	15.3	—	53.1	6.3
		23.00-25.02	94.9	92.1	5.9	3.9	9.0	10.8	26.1	41.5	2.8
4	27.4-33.5	27.60-34.12	95.6	93.1	9.8	3.7	7.7	9.3	—	64.1	5.5
5	33.5-42.7	38.21-41.82	95.8	93.5	5.2	5.8	7.8	11.5	35.8	25.0	9.0
6	42.7-51.8	42.90-49.52	95.6	93.2	9.1	3.1	4.8	13.4	35.8	12.2	21.5
7	51.8-61.0	52.07-60.12	95.8	93.5	12.2	—	10.1	15.5	40.9	—	21.4
8	61.0-70.1	61.14-67.82	94.7	91.7	6.1	—	4.3	11.0	18.3	52.4	7.8
9	70.1-79.2	70.25-76.90	95.9	93.6	3.6	—	5.5	8.2	23.8	51.4	7.6

TABLE 4 – *Continued***Hole 71: < 2μ – *Continued***

Core	Depth	Sample Depth Below Sea Floor (m)	Diff.	Amorph.	Quar.	K-Fe.	Plag.	Kaol.	Mica	Mont.	Bari.
10	79.2-88.4	79.30-87.50	94.8	91.9	4.8	7.1	7.1	11.0	—	61.3	8.6
11	88.4-97.5	91.60-95.20	95.6	93.1	3.3	—	5.3	9.5	16.9	49.2	15.8
12	97.5-106.7	97.73-104.40	95.5	93.0	7.1	—	—	12.7	—	56.0	24.3
13	106.7-115.8	106.80-113.50	96.3	94.2	9.4	8.2	14.5	25.8	—	—	42.0
14	115.8-125.0	116.00-122.60	93.2	89.4	9.1	—	11.2	17.3	—	37.3	25.2
15	125.0-134.1	125.10-131.80	95.8	93.4	12.3	11.4	16.4	20.7	—	—	39.2
16	134.1-143.3	140.65-142.28	94.5	91.4	8.8	—	5.2	12.5	31.7	28.9	12.8
17	143.3-152.4	146.60-151.60	95.0	92.2	10.2	—	4.0	23.2	—	43.2	19.3
18	152.4-161.5	155.00-159.20	95.2	92.5	5.9	3.6	5.6	7.3	33.1	32.0	12.5
19	161.5-170.7	162.25-168.30	96.1	93.9	9.1	—	8.3	12.0	38.7	18.6	13.4
20	170.7-179.8	172.40-179.00	95.1	92.4	5.9	3.0	3.9	11.9	37.8	21.1	16.5
21	179.8-189.0	181.45-188.10	96.3	94.2	4.1	—	5.4	15.4	—	57.7	17.4
22	189.0-198.1	190.80-197.30	94.7	91.7	27.3	—	16.3	22.1	—	—	34.4
23	198.1-207.2	201.20-206.40	94.7	91.7	9.9	2.3	8.8	4.1	37.3	23.4	14.2
24	207.2-216.4	210.30-215.50	93.3	89.6	9.6	2.9	5.3	5.7	26.5	29.8	20.3
25	216.4-225.6	221.00-224.70	94.0	90.7	14.2	4.6	8.8	9.8	—	42.0	20.5
26	225.6-234.7	227.10-233.90	93.7	90.2	8.5	1.1	4.1	5.0	20.0	42.8	18.6
28	243.0-253.0	245.40-252.10	94.6	91.6	13.5	3.5	6.3	10.0	—	36.2	30.4
29	253.0-262.1	253.20-259.80	95.4	92.8	6.3	—	4.6	20.4	49.2	—	19.4
30	262.1-271.3	263.96-270.40	94.2	91.0	3.9	—	—	8.3	53.0	14.3	20.5
31	271.3-280.4	273.02-279.60	93.9	90.5	4.2	—	3.2	—	—	72.7	19.9
32	280.4-289.6	282.10-288.70	91.5	86.7	—	—	7.7	—	36.9	27.5	27.9
33	289.6-298.7	295.80-297.80	94.4	91.3	5.5	9.3	11.8	—	—	—	73.4
34	298.7-307.8	301.45-307.00	95.3	92.7	2.5	5.0	10.7	—	—	52.6	29.2
35	307.0-317.0	309.40-316.20	95.5	93.0	9.2	6.7	11.4	—	—	27.7	45.0
36	317.0-326.1	318.60-325.30	97.4	96.0	3.7	15.4	13.9	—	—	—	67.0
38	335.3-344.4	335.65-343.60	92.6	88.5	1.6	9.6	11.8	—	—	13.1	64.0
39	344.4-353.6	352.10-352.80	93.4	89.7	7.6	—	7.4	—	—	58.2	26.8
40	353.6-362.7	353.91-361.90	92.2	87.8	14.9	4.0	8.4	—	—	34.5	38.3
42	371.9-381.0	372.20-380.20	92.9	88.9	—	2.2	7.2	—	37.5	21.8	31.3
43	381.0-390.1	387.13-389.30	94.2	91.0	3.8	4.8	9.1	—	—	44.8	37.6
44	390.1-399.3	390.17-398.40	100.0	100.0	—	—	—	—	—	—	—
46	408.4-417.6	408.86-416.75	95.2	92.5	5.5	—	14.0	—	—	52.2	28.3
47	417.6-426.7	420.70-425.90	94.2	91.0	8.2	—	16.9	—	—	18.5	56.4
48	426.7-435.9	432.80-435.00	95.1	92.4	9.9	4.2	17.0	27.7	—	—	41.1

**TABLE 5**  
**Results of X-Ray Diffraction Analysis from Site 72**

**Hole 72: Bulk**

Core	Depth	Sample Depth Below Sea Floor (m)	Diff.	Amorph.	Calc.	Mont.
1	0-9.1	0.06-8.40	57.1	33.0	100.0	—
2	59.7-68.9	60.64-67.90	56.8	32.5	100.0	—
3	105.8-114.9	106.01-114.20	55.1	29.8	100.0	—
4	150.0-159.1	150.20-158.30	52.3	25.5	100.0	—
5	210.6-219.8	211.14-219.20	59.8	37.2	100.0	—
6	266.4-275.5	266.63-274.60	51.8	24.7	100.0	—
7	311.8-321.0	311.90-320.00	60.9	38.9	100.0	—
8	321.0-330.1	323.22-329.20	52.3	25.5	100.0	—
9	330.1-339.2	331.65-338.30	53.0	26.6	100.0	—
10	339.2-342.3	340.21-341.92	70.2	53.4	99.1	—
11	342.3-344.1	344.10-344.70	60.3	38.0	97.6	1.8

**Hole 72: 2-20 $\mu$**

Core	Depth	Sample Depth Below Sea Floor (m)	Lithostratigraphy				
			Formation	Unit	Amorph.	Clin.	Bari.
2	59.7-68.9	60.64-67.90	Clipperton	Vari-Colored	93	—	M
3	105.8-114.9	106.01-114.20			86	—	M
5	210.6-219.8	211.14-219.20			87	—	M
6	266.4-275.5	266.63-274.60			86	—	M
7	318.8-321.0	311.90-320.00	Marquesas		75	—	M
8	321.0-330.1	323.22-329.20			96	—	M
9	330.1-339.2	331.65-338.30			83	—	M
10	339.2-342.3	340.21-341.92	Line Islands		92	—	M
11	342.3-344.1	344.10-344.70			88	T	M

**Hole 72: < 2 $\mu$**

Core	Depth	Sample Depth Below Sea Floor (m)	Diff.	Amorph.	Quar.	K-Fe.	Plag.	Kaol.	Mica	Mont.	Bari.	Goet.
			94.8	91.9	6.8	9.6	9.6	11.0	41.2	—	21.7	—
1	0-9.1	0.06-8.40	94.8	91.9	6.8	9.6	9.6	11.0	41.2	—	21.7	—
2	59.7-68.9	60.64-67.90	96.3	94.2	4.0	—	5.4	8.4	30.6	41.4	10.5	—
3	105.8-114.9	106.01-114.20	96.2	94.1	—	—	26.3	—	—	—	73.7	—
4	150.0-159.1	150.20-158.30	100.0	100.0	—	—	—	—	—	—	—	—
5	210.6-219.8	211.14-219.20	93.7	90.2	6.5	2.0	2.6	—	36.1	30.6	22.2	—
6	266.4-275.5	266.63-274.60	94.4	91.3	2.3	—	2.9	—	—	94.8	—	—

TABLE 5 – *Continued***Hole 72: < 2μ – *Continued***

Core	Depth	Sample Depth Below Sea Floor (m)	Diff.	Amorph.	Quar.	K-Fe.	Plag.	Kaol.	Mica	Mont.	Bari.	Goet.
7	311.8-321.0	311.90-320.00	92.0	87.5	5.9	2.2	7.2	5.8	55.9	14.7	8.4	—
8	321.0-330.1	323.22-329.20	92.8	88.8	8.7	13.0	8.2	17.0	—	53.1	—	M
9	330.1-339.2	331.65-338.30	92.7	88.6	5.2	—	5.2	3.8	30.7	47.6	7.5	—
10	339.2-342.3	340.21-341.92	93.5	89.9	4.8	—	9.9	5.2	43.3	30.6	6.3	—
11	342.3-344.1	344.10-344.70	92.6	88.5	5.2	4.0	7.1	5.9	—	71.2	6.6	—

**Hole 72A: Bulk**

Core	Depth	Sample Depth Below Sea Floor (m)	Diff.	Amorph.	Calc.
1	9.1-18.3	10.24-14.31	56.9	32.7	99.6
2	18.3-27.4	18.40-25.10	70.8	54.4	99.4
3	27.4-36.6	28.98-35.50	56.2	31.6	100.0
4	36.6-45.7	36.90-40.30	63.2	42.5	100.0
		41.52	63.4	42.8	99.4
		43.40	60.3	38.0	100.0
		44.73	65.3	45.8	99.4
5	45.7-54.9	46.34-53.90	57.8	34.1	100.0
6	54.9-64.0	55.00-63.10	54.8	29.4	100.0

**Hole 72A: 2-20μ**

Core	Depth	Sample Depth Below Sea Floor (m)	Lithostratigraphy			
			Formation	Unit	Amorph.	Bari.
1	9.1-18.3	10.24-14.31		Cyclic	95	M
2	18.3-27.4	18.40-25.10			93	M
3	27.4-36.6	28.98-35.50			95	M
4	36.6-45.7	36.90-40.30	Cliperton		95	M
		41.52			99	M
		43.40			99	—
		44.73			99	M
5	45.7-54.9	46.34-53.90	Varicolored		95	M
6	54.9-64.0	55.00-63.10			94	M

TABLE 5 – *Continued*

Hole 72A: &lt;2μ

Core	Depth	Sample Depth Below Sea Floor (m)	Diff.	Amorph.	Quar.	K-Fe.	Plag.	Kaol.	Mica	Mont.	Bari.
2	18.3-27.4	18.40-25.10	96.5	94.6	4.5	9.2	8.0	9.9	37.9	24.0	6.6
4	36.6-45.7	36.90-40.30	96.0	93.8	18.3	—	31.0	—	—	31.5	19.2
		41.52	96.7	94.9	13.9	5.2	16.6	13.9	50.4	—	—
		43.40	96.1	93.9	9.9	3.9	9.6	9.4	31.1	27.7	8.6
5	45.7-54.9	43.34-53.90	100.0	100.0	—	—	—	—	—	—	—

**TABLE 6**  
Results of X-Ray Diffraction Analysis from Site 73

**Hole 73: Bulk**

Core	Depth	Sample Depth Below Sea Floor (m)	%									
			Diff.	Amorph.	Calc.	Quar.	Plag.	Kaol.	Mica	Mont.	Phil.	Bari.
1	0-3	0.05-2.40	56.1	31.4	100.0	—	—	—	—	—	—	—
2	3-12.2	4.65-11.20	55.0	29.7	100.0	—	—	—	—	—	—	—
3	12.2-21.3	13.90-16.80	56.3	31.7	100.0	—	—	—	—	—	—	—
		17.50-20.30	59.3	36.4	100.0	—	—	—	—	—	—	—
4	21.3-30.5	21.40-29.65	57.4	33.4	100.0	—	—	—	—	—	—	—
5	30.5-39.6	31.65-38.70	60.2	37.8	100.0	—	—	—	—	—	—	—
6	39.6-48.8	39.70-47.80	65.6	46.2	100.0	—	—	—	—	—	—	—
7	48.8-57.9	48.90-49.70	66.0	46.9	100.0	—	—	—	—	—	—	—
		52.20-57.10	70.8	54.4	99.4	—	—	—	—	—	—	—
8	57.9-67.1	58.00-61.60	67.3	48.9	94.0	—	5.4	—	—	—	—	—
		62.50	77.4	64.7	91.7	—	—	—	—	5.6	—	2.3
		63.50	82.9	73.3	80.6	—	2.6	1.5	9.5	—	—	5.0
		64.00	61.4	39.7	99.1	—	—	—	—	—	—	—
		64.90	90.3	84.8	58.9	2.6	13.5	11.0	—	—	—	14.0
		65.50-65.86	86.2	78.4	64.5	1.6	—	—	10.2	—	17.3	6.4
9	67.1-76.2	67.90-75.30	70.6	54.1	93.8	—	—	—	—	2.9	—	2.4
10	76.2-85.3	76.20-84.40	56.7	32.3	96.1	—	—	—	—	3.4	—	—
11	85.3-94.5	85.50-93.50	56.9	32.7	97.0	—	—	—	—	2.5	—	—
12	139.9-149.0	140.00-148.10	51.3	23.9	100.0	—	—	—	—	—	—	—
13	206.0-215.2	206.10-214.20	50.5	22.7	100.0	—	—	—	—	—	—	—
14	242.6-251.8	242.70-250.80	50.8	23.1	100.0	—	—	—	—	—	—	—
15	251.8-260.9	252.50-260.00	50.9	23.3	100.0	—	—	—	—	—	—	—
16	260.9-270.1	261.00-269.10	52.0	25.0	100.0	—	—	—	—	—	—	—
17	270.1-279.2	270.40-278.30	53.7	27.7	100.0	—	—	—	—	—	—	—
18	279.2-288.3	283.80-287.40	54.1	28.3	100.0	—	—	—	—	—	—	—
19	288.3-297.5	288.50-296.50	69.0	51.6	97.3	1.4	1.3	—	—	—	—	—
20	297.5-300.5	297.50-299.88	61.0	39.1	99.6	—	—	—	—	—	—	—
21	300.5-303.0	300.65	56.1	31.4	96.6	—	—	—	—	3.0	—	—

**Hole 73: 2-20 $\mu$**

Core	Depth	Sample Depth Below Sea Floor (m)	Lithostratigraphy			
			Formation	Unit	Amorph.	Bari.
1	0-3.0	0.05-2.40		Cyclic	99	M
2	3.0-12.2	4.65-11.20			97	M
3	12.2-21.3	13.90-16.80			96	M

TABLE 6 – *Continued***Hole 73: 2-20 $\mu$  – *Continued***

Core	Depth	Sample Depth Below Sea Floor (m)	Lithostratigraphy			
			Formation	Unit	Amorph.	Bari.
		17.50-20.30			98	M
4	21.3-30.5	21.40-29.65			99	M
5	30.5-39.6	31.65-38.70			98	M
6	39.6-48.8	39.70-47.80			97	M
7	48.8-57.9	48.90-49.70			100	M
		52.20-57.10			97	M
8	57.9-67.1	58.00-61.60			98	M
		62.50			100	—
		63.50			99	M
		64.00			98	M
		64.90			98	M
		65.50-65.86	Clipperton	Varicolored	95	M
9	67.1-76.2	67.90-75.30			94	M
10	76.2-85.3	76.20-84.40			95	M
11	85.3-94.5	85.50-93.50			92	M
12	139.9-149.0	140.00-148.10			87	M
13	206.0-215.2	206.10-214.20			88	M
14	242.6-251.8	242.70-250.80			92	M
15	251.8-260.9	252.50-260.00			93	M
16	260.9-270.1	261.00-269.10			95	M
17	270.1-279.2	270.40-278.30	Line Islands		97	M
18	279.2-288.3	283.80-287.40			98	M
19	288.3-297.5	288.50-296.50			95	M
20	297.5-300.5	297.50-299.88			95	M
21	300.5-303.0	300.65			97	—

**Hole 73: < 2 $\mu$** 

Core	Depth	Sample Depth Below Sea Floor (m)	Lithostratigraphy								
			Diff.	Amorph.	Quar.	K-Fe.	Plag.	Kaol.	Mica	Mont.	Bari.
1	0-3	0.05-2.40	100.0	100.0	—	—	—	—	—	—	—
2	3.0-12.2	4.65-11.20	97.5	96.1	28.0	—	26.9	37.1	—	—	8.0
3	12.2-21.3	13.90-16.80	97.2	95.7	22.6	—	29.7	31.0	—	—	16.8
		17.50-20.30	95.3	92.7	5.0	—	13.8	21.0	51.3	—	8.8
4	21.3-30.5	21.40-29.65	95.6	93.1	6.1	—	12.9	14.1	36.8	21.2	9.0
5	30.5-39.6	31.65-38.70	95.5	93.0	—	—	10.7	—	—	76.1	13.2
6	39.6-48.8	39.70-47.80	100.0	100.0	—	—	—	—	—	—	—

TABLE 6 – *Continued***Hole 73: < 2μ – *Continued***

Core	Depth	Sample Depth Below Sea Floor (m)									
			Diff.	Amorph.	Quar.	K-Fe.	Plag.	Kaol.	Mica	Mont.	Bari.
7	48.8-57.9	48.90-49.70	95.5	93.0	7.8	10.7	6.7	—	—	62.0	12.8
		52.20-57.10	96.5	94.5	17.1	—	29.0	37.8	—	—	16.1
8	57.9-67.1	58.00-61.60	100.0	100.0	—	—	—	—	—	—	—
		62.50	95.1	92.3	2.8	9.7	11.8	—	—	71.5	4.3
		63.50	100.0	100.0	—	—	—	—	—	—	—
		64.00	100.0	100.0	—	—	—	—	—	—	—
		64.90	95.0	92.2	14.9	—	38.6	—	—	—	46.4
		65.50-65.86	95.1	92.4	5.1	—	9.0	19.7	—	57.9	8.3
9	67.1-76.2	67.90-75.30	94.4	91.3	5.4	7.0	8.6	10.2	—	62.7	6.1
10	76.2-85.3	76.20-84.40	94.4	91.3	—	—	8.8	8.3	—	73.6	8.6
11	85.3-94.5	85.50-93.50	94.1	90.8	3.5	—	12.7	18.0	56.8	—	9.0
12	139.9-149.0	140.00-148.10	94.3	91.1	7.1	—	13.1	15.4	32.4	23.4	8.6
13	206.0-215.2	206.10-214.20	94.5	91.4	3.2	—	6.8	5.9	24.9	50.2	9.1
14	242.6-251.8	242.70-250.80	93.0	89.0	10.4	—	6.7	9.2	69.9	—	3.8
15	251.8-260.9	252.50-260.00	93.8	90.3	6.2	—	9.0	9.8	69.4	—	5.6
16	260.9-270.1	261.00-269.10	92.9	88.9	9.5	—	5.1	10.3	71.0	—	4.1
17	270.1-279.2	270.40-278.30	95.1	92.4	7.4	—	8.0	6.2	69.8	—	8.6
18	279.2-288.3	283.80-287.40	94.7	91.7	9.9	—	7.6	11.6	62.6	—	8.3
19	288.3-297.5	288.50-296.50	95.4	92.8	3.5	—	22.1	—	55.1	—	19.2
20	297.5-300.5	297.50-299.88	92.7	88.6	6.0	—	7.3	4.0	32.8	48.5	1.4
21	300.5-303.0	300.65	93.3	89.6	3.2	—	5.3	13.0	24.1	54.4	—

**TABLE 7**  
**Results of X-Ray Diffraction Analysis from Site 74**

**Hole 74: Bulk**

Core	Depth	Sample Depth Below Sea Floor (m)	Sample Depth Below Sea Floor										
			Diff.	Amorph.	Calc.	Quar.	Plag.	Kaol.	Mica	Mont.	Clin.	Phil.	Bari.
1	0.9-1.1	0.75-8.40	94.9	92.0	—	2.8	32.0	—	35.1	24.0	—	—	6.1
2	9.1-18.3	14.65-16.70	94.3	91.1	—	9.0	—	—	—	—	—	—	83.3
		17.78	69.3	52.0	98.8	—	—	—	—	—	—	—	—
3	18.3-27.4	20.70-22.40	93.3	89.5	15.6	5.2	2.2	2.4	14.8	17.6	—	37.2	4.9
		22.90-26.70	69.3	52.0	98.3	—	1.0	—	—	—	—	—	—
4	27.4-36.6	29.15	93.1	89.2	—	11.9	6.5	10.3	33.5	—	—	33.5	4.4
		29.65-35.65	60.9	38.9	100.0	—	—	—	—	—	—	—	—
5	36.6-45.7	36.90-44.20	62.4	41.2	100.0	—	—	—	—	—	—	—	—
6	45.7-54.9	45.80-54.10	63.1	42.3	99.7	—	—	—	—	—	—	—	—
7	54.9-64.0	55.70-61.00	64.7	44.8	99.7	—	—	—	—	—	—	—	—
8	64.0-73.2	68.60-70.90	61.4	39.7	100.0	—	—	—	—	—	—	—	—
9	73.2-82.3	73.80-81.45	60.7	38.6	100.0	—	—	—	—	—	—	—	—
10	82.3-91.4	88.60-91.10	61.9	40.5	100.0	—	—	—	—	—	—	—	—
11	91.4-100.6	99.60	61.4	39.7	100.0	—	—	—	—	—	—	—	—
		100.14	64.3	44.2	99.2	—	—	—	—	—	—	—	—
12	100.6-102.4	100.70	80.3	69.2	65.9	5.0	—	—	14.2	—	1.1	13.9	—
		100.35-102.60	81.1	70.5	99.2	—	—	—	—	—	—	—	—

**Hole 74: 2-20 $\mu$**

Core	Depth	Sample Depth Below Sea Floor (m)	Lithostratigraphy						
			Formation	Unit	Amorph.	Clin.	Phil.	Bari.	Goet.
1	0.9-1.1	0.75-8.40			95	—	—	—	—
2	9.1-18.3	14.65-16.70			98	—	M	—	—
		17.78	Clipperton	Radiolarian ooze	98	—	M	—	—
3	18.3-27.4	20.70-22.40			94	—	M	—	—
		22.90-26.70			94	—	M	—	—
4	27.4-36.6	29.15			92	—	M	—	—
		29.65-35.65			93	—	—	M	—
5	36.6-45.7	36.90-44.20			70	—	—	—	—
7	54.9-64.0	55.70-61.00			85	—	—	—	—
8	64.0-73.2	68.60-70.90			75	M	—	—	—
9	73.2-82.3	73.80-81.45			84	M	—	P	—
10	82.3-91.4	88.60-91.10			92	M	—	—	—
11	91.4-100.6	99.60			99	M	—	—	—
		100.14	Marquesas	Line Islands	72	M	M	—	—
12	100.6-102.4	100.70			78	P	M	—	P
		100.35-102.60			88	—	—	—	M

TABLE 7 – *Continued*Hole 74: < 2 $\mu$ 

Core	Depth	Sample Depth Below Sea Floor (m)											
			Diff.	Amorph.	Quar.	Plag.	Kaol.	Mica	Chlo.	Mont.	Clin.	Phil.	Goe
1	0-9.1	0.75-8.40	95.2	92.5	4.1	23.5	8.2	—	—	64.2	—	—	—
2	9.1-18.3	14.65-16.70	94.8	91.9	4.9	18.6	14.7	61.8	—	—	—	—	—
		17.78	98.1	97.1	50.2	—	49.8	—	—	—	—	—	—
3	18.3-27.4	20.70-22.40	95.0	92.2	6.1	14.3	14.9	39.2	—	25.5	—	—	—
		22.90-26.70	93.7	90.2	6.1	10.8	6.4	21.6	—	55.0	—	—	—
4	27.4-36.6	29.15	93.4	89.7	9.2	—	—	21.0	—	48.9	—	21.0	—
		29.65-35.65	93.9	90.5	3.7	4.9	5.5	27.0	—	58.9	—	—	—
5	36.6-45.7	36.90-44.20	93.3	89.6	4.4	3.2	3.2	26.8	—	62.4	—	—	—
6	45.7-54.9	45.80-54.10	90.4	85.0	12.6	1.6	4.1	30.7	—	10.0	2.5	38.6	—
7	54.9-64.0	55.70-61.00	94.4	91.3	5.8	5.6	—	34.2	2.8	51.4	—	—	—
8	64.0-73.2	68.60-70.90	95.2	92.5	3.8	4.4	5.8	70.6	—	9.7	5.8	—	—
10	82.3-91.4	88.60-91.10	97.9	96.7	8.8	—	—	—	—	91.2	—	—	—
11	91.4-100.6	99.60	97.5	96.1	6.5	4.6	—	31.5	—	57.4	—	—	—
		100.14	93.6	90.0	8.7	10.5	12.4	68.4	—	—	—	—	—
12	100.6-102.4	100.70	91.4	86.6	7.6	6.7	5.0	26.2	—	52.5	2.0	—	—
		100.35-102.60	89.9	84.2	100.0	—	—	—	—	—	—	—	M

**TABLE 8**  
**Results of X-Ray Diffraction Analysis from Site 75**

**Hole 75: Bulk**

Core	Depth	Sample Depth Below Sea Floor (m)	Diff.	Amorph.	Calc.	Quar.	Mica	Phil.
1	0.9-1	0.20-0.63	88.4	81.9	—	3.7	21.0	75.3
		1.50-3.70	66.1	47.0	97.5	—	—	2.5
		4.30-5.80	62.0	40.6	100.0	—	—	—
2	9.1-18.3	9.15-15.80	61.6	40.0	100.0	—	—	—
3	18.3-27.4	19.20-26.50	62.1	40.8	100.0	—	—	—
4	27.4-36.6	27.75-35.60	61.8	40.3	100.0	—	—	—
5	36.6-45.7	36.75-44.80	62.7	41.7	100.0	—	—	—
7	54.9-64.0	55.70-59.80	63.4	42.8	100.0	—	—	—
8	64.0-73.2	64.05-72.20	63.3	42.7	100.0	—	—	—
9	73.2-81.7	73.45	62.1	40.8	100.0	—	—	—
		74.30-81.40	67.0	48.4	100.0	—	—	—

**Hole 75: 2-20μ**

Core	Depth	Sample Depth Below Sea Floor (m)	Lithostratigraphy					
			Formation	Unit	Amorph.	Clin.	Phil.	Goet.
1	0.9-1	0.20-0.63	Residuum	—	67	—	M	P
		1.50-3.70		—	78	—	M	P
		4.30-5.80		—	77	—	M	P
2	9.1-18.3	9.15-15.80	Marquesas	—	87	—	M	P
3	18.3-27.4	19.20-26.50		—	68	—	M	—
4	27.4-36.6	27.75-35.60		—	85	—	P	P
5	36.6-45.7	36.75-44.80		—	69	P	M	P
7	54.9-64.0	55.70-59.80		—	85	P	—	M
8	64.0-73.2	64.05-72.20		—	84	P	—	M
9	73.2-81.7	73.45		—	78	—	M	—
		74.30-81.40		—	88	—	—	M

**Hole 75: < 2μ**

Core	Depth	Sample Depth Below Sea Floor (m)	Diff.	Amorph.	Quar.	Plag.	Kaol.	Mica	Phil.	Goet.
1	0.9-1	0.20-0.63	92.7	88.6	6.0	16.4	—	36.0	41.6	M
		1.50-3.70	91.4	86.6	40.8	59.2	—	—	—	P
		4.30-5.80	91.6	86.9	20.0	43.4	36.6	—	—	P
2	9.1-18.3	9.15-15.80	92.5	88.3	6.7	3.8	11.0	54.6	23.8	P

TABLE 8 – *Continued***Hole 75: < 2μ – *Continued***

Core	Depth	Sample Depth Below Sea Floor (m)	Diff.	Amorph.	Quar.	Plag.	Kaol.	Mica	Phil.	Goet.
3	18.3-27.4	19.20-26.50	91.4	86.6	7.1	—	5.4	45.0	42.5	P
4	27.4-36.6	27.75-35.60	91.8	87.2	7.1	—	5.4	45.0	42.5	P
5	36.6-45.7	36.75-44.80	90.8	85.7	6.7	—	16.8	76.4	—	P
7	54.9-64.0	55.70-59.80	89.3	83.3	8.6	—	10.3	81.1	—	P
8	64.0-73.2	64.05-72.20	90.8	85.7	100.0	—	—	—	—	P
9	73.2-81.7	73.45	93.5	89.8	3.9	—	5.8	48.8	41.5	—